Cluster Output Synchronization for Memristive Neural Networks

Chao Zhou[a], Chunhua Wang[a,*], Yichuang Sun[b], Wei Yao[a], Hairong Lin[a]

[a]*College of Information Science and Engineering, Hunan University, Changsha 410082, China*
[b]*School of Engineering and Technology, University of Hertfordshire, Hatfield AL10 9AB, U.K*

Abstract

Herein, cluster output synchronization for memristive neural networks (MNNs) is investigated using two different control schemes. Existing synchronization models for MNNs focus on the behavior of a single neuron node in one-cluster networks. However, actual neural networks (NNs) are clustered organizations consisting of multiple interacting clusters, where the nodes from the same cluster combine and work together. This study proposes a cluster output synchronization model for MNNs, which considers the combination output behavior of the nodes in NNs clusters. Accordingly, two specific control schemes are designed: one based on feedback control involves designing a small number of controllers to reduce control costs, and the other based on adaptive control involves designing multiple adjustable controllers to increase the anti-interference capacity of the control system. Meanwhile, to facilitate synchronization in MNNs, a model relationship between MNNs and traditional NNs is investigated. By utilizing the control schemes, model relationship, and Lyapunov stability theory, sufficient conditions are obtained for validating the cluster output synchronization. Finally, several numerical examples are given to illustrate the accuracy of the theoretical results.

Keywords: cluster synchronization, memristive neural networks, model relationship, output synchronization

1. Introduction

Before the memristor was discovered in 1971, through the relationship between charge and magnetic flux, Chua theoretically inferred the existence of a basic circuit component in addition to the resistor, capacitor, and inductor [1]. Thirty-seven years later, Hewlett-Packard Company successfully validated Chua's theory by making the first memristive nanometer device [2]. Subsequently, it has been successfully applied in various fields owing to its excellent characteristics, such as low power consumption, good scalability, and nonvolatile memory [3–5]. A breakthrough application would be to establish a memristive neural network model because memristor can accurately mimic real synapsis. Compared to traditional NNs, MNNs have more complex and richer dynamics behaviors and can better simulate real nervous systems. Thus, many studies on the dynamics characteristics of MNNs have been published [6–8].

As a type of primary collective behavior, synchronization can be widely observed in many natural environments and complex systems. In recent years, synchronization of complex networks has attracted a lot of research attention due to its applicability to associative memory [9], brain science [10], information encryption [11], combinatorial optimization [12] and so on. Notably, many studies into the synchronization of MNNs have also been conducted because synchronization behavior is pivotal to some important NNs functions (e.g., information expression [13] and pattern recognition [14]). In [15], the authors explored quasi-synchronization for a class of chaotic MNNs, which were treated as the NNs with indeterminate coefficients, and a feedback control strategy was employed to realize synchronization. In [16], Li et al. considered the MNNs with parameter mismatch and derived some sufficient conditions for lag synchronization by utilizing the Halanay inequality and ω-Measure method. By applying weighted double-integral inequalities and Lyapunov stability theory, Feng et al. studied asymptotic synchronization for MNNs

*Corresponding author
Email address: wch1227164@hnu.edu.cn (Chunhua Wang)

with mixed delay under quantized intermittent control [17]. More studies could be found in [18–22] and the references therein.

Synchronization can be divided into various models depending on the characteristics of collective dynamical behaviors: cluster synchronization, finite-time synchronization, fixed-time synchronization, asymptotic synchronization and output synchronization . Among them, cluster synchronization is unique. It can be observed when the ensemble of a network divides into several portions where the nodes within one portion are synchronous, whereas those from different portions are not. Because cluster synchronization behavior is common across many natural and science systems [23], and has a wide range of applications, cluster synchronization of complex networks, including traditional NNs, has been extensively studied [24–29]. For instance, Zhou et al. applied an adaptive pinning control strategy to handle cluster synchronization problem of complex networks with diverse dynamics nodes and stochastic disturbances [24]. In [25], the authors simultaneously dealt with fixed-time and finite-time synchronization for complex networks with interacting clusters in the cases with and without pinning control, and synchronization settling time was estimated by applying theories on finite-time stability. In [26], a type of traditional NNs with hybrid coupled term and delay was studied and cluster synchronization was achieved by utilizing a matrix-based method. In [27], the authors further researched the main results of [26] and extended early finding to a type of stochastic delayed NNs. However, cluster synchronization for MNNs has not yet been reported, which remains as an open challenge.

In accordance with the model structure, current synchronization models for MNNs, such as the ones in [15–22], can almost be sorted into a type of node-to-node synchronization pattern, as illustrated in Fig.1. The node within the response system attempts to synchronize with the according node within the drive system via a controller. Such a pattern focuses on the behavior of a single node in a network containing one cluster, while it may be monotonous and insufficient for NNs study. On the one hand, although it is feasible to control neuron node states for synchronization by applying neural electrode tools [30], many neuron nodes in NNs are usually present, and successfully controlling each node is unlikely and difficult. On the other hand, NNs consist of multiple structured clusters, where the nodes belonging to the same cluster share morphological and functional similarities, and always combine and work together for function implementations [31, 32]. Thus, combination behaviors of neuron nodes within clusters, such as the weighted sum of node states [33], have a more direct and significant effect on function than single node behavior. For instance, in some NNs studies on information expression and processing mechanism [34, 35], it was demonstrated that accurate and complete information expression in NNs is based on the weighted sum of node states in populations (i.e., clusters). In contrast, the single node state only presents limited and rough information. Therefore, to elucidate the synchronization activities of NNs [13, 14], it is necessary to consider the combination behavior of neuron nodes in NNs clusters.

Accordingly, this article proposes a cluster output synchronization model for MNNs, as demonstrated in Fig. 2 where the weighted sums of node states in clusters are expressed as the cluster outputs, and the synchronization is realized between the outputs of the drive and response systems. The main contributions of this study are summarized below.

1) A cluster output synchronization model for MNNs (and NNs) is presented for the first time. It differs from the existing node-to-node synchronization models and provides a more practical model structure for MNNs. Moreover, it

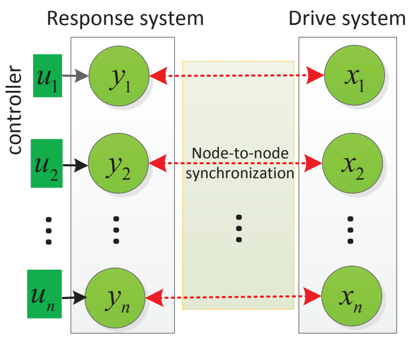

Figure 1: Node-to-node synchronization model for MNNs.

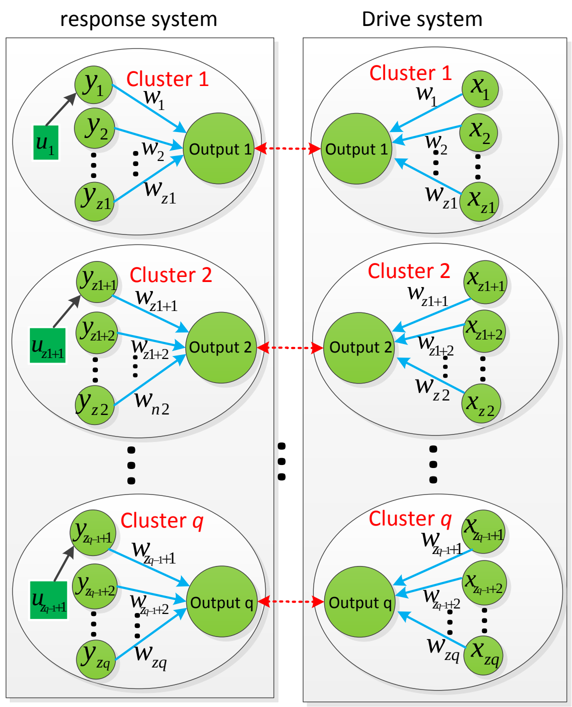

Figure 2: Cluster output synchronization model for MNNs where $w_i, i = 1, 2, \cdots, z_q$ denote output weights.

is more general since it can be reduced to the node-to-node model in the special case that there exists only one node in each cluster, which can be observed in Fig. 2.

2) To study synchronization in MNNs, a model relationship between MNNs and traditional NNs is investigated by employing differential inclusion and measurable function theories.

3) Two specific control schemes are designed for the proposed synchronization model, where one scheme aims to reduce control costs by designing a small number of fixed feedback controllers, whereas the other is designed to increase the anti-interference capacity in control system using adjustable adaptive controllers. Utilizing the control schemes, model relationship, and Lyapunov stability theory, some sufficient conditions are then obtained to ensure cluster output synchronization.

Notations: Throughout this article, $\mathrm{diag}(a_1, a_2, ..., a_n)$ denotes a diagonal matrix of n-dimension. For a matrix A, A^T and A^{-1} stand for the transpose and the inverse of A, respectively. $\|\cdot\|$ represents the standard 2-norm of a matrix or vector. Let $\varepsilon > 0$, $C([-\varepsilon, 0], \mathbb{R})$ stands for the family of continuous functions from $[-\varepsilon, 0]$ to $\mathbb{R}$. I_n represents the n-dimensional identity matrix. 1_n denotes the all-one column vector in $\mathbb{R}^n$.

2. Preliminaries

In this article, we consider a directed network with a set of nodes $\nu = \{1, 2, ..., D\}$ and assume that it can be split into q nonempty clusters, represented by $\nu_1, \nu_2, ..., \nu_q$ which satisfy $\cup_{\ell=1}^{q} \nu_\ell = \nu$. For convenience, let N_ℓ denote the number of ℓth cluster ν_ℓ and $Z_\ell = \sum_{J=1}^{\ell} N_J$. Then, it is expressible that $\nu_\ell = \{Z_{\ell-1} + 1, Z_{\ell-1} + 2, ..., Z_\ell\}$, where $Z_0 = 0$. Additionally, for $j \in \nu_\ell$, let $\bar{j}$ denote the subscript of ℓth cluster, i.e., $\bar{j} = \ell$ if $j \in \nu_\ell$.

Consider the following MNNs with multiple clusters and time-varying delay, whose dynamic equation can be described by

$$\dot{x}_i(t) = -s_i x_i(t) + \sum_{j=1}^{Z_q} \psi_{ij}(x_i(t)) f_{\bar{j}}(x_j(t)) + \sum_{j=1}^{Z_q} \phi_{ij}(x_i(t)) g_{\bar{j}}(x_j(t - \varepsilon_{\bar{j}}(t))) + I_i, \quad i \in \nu_\ell, \ell = 1, ..., q \tag{1}$$

where $s_i > 0$ represents the self-inhibition, $f_{\bar{j}}(\cdot)$ and $g_{\bar{j}}(\cdot)$ denote the activation functions in $\bar{j}$th cluster, $\varepsilon_{\bar{j}}(t)$ stands for the transmission delay in $\bar{j}$th cluster and meets $0 < \varepsilon_{\bar{j}}(t) \le \varepsilon_{\bar{j}}$, where $\varepsilon_{\bar{j}} > 0$ is a constant. I_i is the outside input. $\psi_{ij}(x_i(t))$ and $\phi_{ij}(x_i(t))$ are the memristive connection weights, and based on the simplified mathematical model of memristor, we can describe them as follows:

$$\psi_{ij}(x_i(t)) = \begin{cases} \overleftarrow{\psi}_{ij}, |x_i(t)| \le T_i \\ \vec{\psi}_{ij}, |x_i(t)| > T_i \end{cases} \tag{2}$$

$$\phi_{ij}(x_i(t)) = \begin{cases} \overleftarrow{\phi}_{ij}, |x_i(t)| \le T_i \\ \vec{\phi}_{ij}, |x_i(t)| > T_i \end{cases} \tag{3}$$

where switching jumps $T_i > 0$, $\overleftarrow{\psi}_{ij}, \vec{\psi}_{ij}$, $\overleftarrow{\phi}_{ij}$ and $\vec{\phi}_{ij}$ are some constants. The initial values of (1) are denoted as $x_i(a) = G_i(a)$, $a \in [-\varepsilon_{\bar{i}}, 0]$, and $G_i(a) \in C([-\varepsilon_{\bar{i}}, 0], \mathbb{R})$, $i \in \nu_\ell, \ell = 1,...,q$.

Viewing (1) as drive system, response system that aims to synchronize with (1) is

$$\dot{y}_i(t) = -s_i y_i(t) + \sum_{j=1}^{Z_q} \psi_{ij}(y_i(t)) f_{\bar{j}}(y_j(t)) + \sum_{j=1}^{Z_q} \phi_{ij}(y_i(t)) g_{\bar{j}}(y_j(t - \varepsilon_{\bar{j}}(t))) + u_i + I_i, \quad i \in \nu_\ell, \ell = 1,...,q \tag{4}$$

where $\psi_{ij}(y_i(t))$ and $\phi_{ij}(y_i(t))$ are defined similarly to (2) and (3), respectively. u_i is the controller to be designed. In general, the initial values of (4) are different from those of (1) and denoted by $y_i(a) = F_i(a)$, $a \in [-\varepsilon_{\bar{i}}, 0]$ and $F_i(a) \in C([-\varepsilon_{\bar{i}}, 0], \mathbb{R})$, $i \in \nu_\ell, \ell = 1,...,q$.

In light of equalities (2) and (3), it is observed that MNNs are a type of discontinuous state-dependent switching system. Thus, the solutions of the systems (1), (4) will be handled in Filippovs sense. In the following, we give the relevant definition.

Definition 1 ([36]): The Filippov set-valued map of $g(t, x)$ at $x \in \mathbb{R}^n$ is defined as

$$G(t, x) = \bigcap_{\delta > 0} \bigcap_{\mu(N) = 0} \overline{\text{co}}[f(B(x, \partial) \backslash N)]$$

where $\overline{\text{co}}[\cdot]$ represents the closure of the convex hull, $B(x, \partial)$ denotes the ball of center x and radius ∂, and $\mu(N)$ denotes the Lebesgue measure of set N.

Let $\psi^*_{ij} = \min\left\{\overleftarrow{\psi}_{ij}, \vec{\psi}_{ij}\right\}$, $\psi^{**}_{ij} = \max\left\{\overleftarrow{\psi}_{ij}, \vec{\psi}_{ij}\right\}$, $\phi^*_{ij} = \min\left\{\overleftarrow{\phi}_{ij}, \vec{\phi}_{ij}\right\}$, $\phi^{**}_{ij} = \max\left\{\overleftarrow{\phi}_{ij}, \vec{\phi}_{ij}\right\}$, $\psi_{ij} = \frac{\psi^{**}_{ij} + \psi^*_{ij}}{2}$, $\Delta\psi_{ij} = \frac{\psi^{**}_{ij} - \psi^*_{ij}}{2}$, $\phi_{ij} = \frac{\phi^{**}_{ij} + \phi^*_{ij}}{2}$, $\Delta\phi_{ij} = \frac{\phi^{**}_{ij} - \phi^*_{ij}}{2}$.

Then, based on Definition 1 and by utilizing differential inclusion and measurable function theories [37], the system (1) can be rewritten as

$$\dot{x}_i(t) = -s_i x_i(t) + \sum_{j=1}^{Z_q} (\psi_{ij} + \Delta\psi_{ij} \varsigma^1_{ij}(t)) f_{\bar{j}}(x_j(t)) + \sum_{j=1}^{Z_q} (\phi_{ij} + \Delta\phi_{ij} \varsigma^2_{ij}(t)) g_{\bar{j}}(x_j(t - \varepsilon_{\bar{j}}(t))) + I_i, \quad \ell = 1,...,q.$$

where $\varsigma^1_{ij}(t) \in \overline{co}[-1, 1]$ and $\varsigma^2_{ij}(t) \in \overline{co}[-1, 1]$ are measurable functions.

For convenience, denote

$$\partial^x_i(t) = \sum_{j=1}^{Z_q} \Delta\psi_{ij} \varsigma^1_{ij}(t) f_{\bar{j}}(x_j(t)) + \sum_{j=1}^{Z_q} \Delta\phi_{ij} \varsigma^2_{ij}(t) g_{\bar{j}}(x_j(t - \varepsilon_{\bar{j}}(t)))$$

and one has

$$\dot{x}_i(t) = -s_i x_i(t) + \sum_{j=1}^{Z_q} \psi_{ij} f_{\bar{j}}(x_j(t)) + \sum_{j=1}^{Z_q} \phi_{ij} g_{\bar{j}}(x_j(t - \varepsilon_{\bar{j}}(t))) + \partial^x_i(t) + I_i, \quad i \in \nu_\ell, \ell = 1,...,q. \tag{5}$$

Analogously, it can be deduced from the system (4) that

$$\dot{y}_i(t) = -s_i y_i(t) + \sum_{j=1}^{Z_q} \psi_{ij} f_{\bar{j}}(y_j(t)) + \sum_{j=1}^{Z_q} \phi_{ij} g_{\bar{j}}(y(t-\varepsilon_{\bar{j}}(t))) + \partial_i^y(t) + u_i + I_i, \quad i \in \nu_\ell, \ell = 1,...,q \tag{6}$$

where $\partial_i^y(t) = \sum_{j=1}^{Z_q} \Delta\psi_{ij}\varsigma_{ij}^3(t) f_{\bar{j}}(y_j(t)) + \sum_{j=1}^{Z_q} \Delta\phi_{ij}\varsigma_{ij}^4(t) g_{\bar{j}}(y(t-\varepsilon_{\bar{j}}(t)))$, and $\varsigma_{ij}^3(t) \in \overline{co}[-1,1]$ and $\varsigma_{ij}^4(t) \in \overline{co}[-1,1]$ are some measurable functions.

Remark 1: By applying the differential inclusion and measurable selection theories, memristive connection coefficients can be divided into two portions. Then, we can separate the terms $\partial_i^x(t)$ and $\partial_i^y(t)$ $(i \in \nu_\ell, \ell = 1,...,q)$ in the systems (5) and (6). It can be seen from the definitions of $\partial_i^x(t)$ and $\partial_i^y(t)$ that they reflect the coefficient jumps caused by memristor. The rest coupling portions including $\sum_{j=1}^{Z_q} \psi_{ij} f_{\bar{j}}(x_j(t))$, $\sum_{j=1}^{Z_q} \phi_{ij} g_{\bar{j}}(x_j(t-\varepsilon_{\bar{j}}(t)))$, $\sum_{j=1}^{Z_q} \psi_{ij} f_{\bar{j}}(y_j(t))$ and $\sum_{j=1}^{Z_q} \phi_{ij} g_{\bar{j}}(y_j(t-\varepsilon_{\bar{j}}(t)))$ $(i \in \nu_\ell, \ell = 1,...,q)$ have constant connection coefficients and are similar to the coupling forms in traditional NNs [38–40]. Thus, some approaches developed in these researches can be utilized to efficiently tackle these portions in the later work. Such a transformation helps to build a model relationship between traditional NNs and MNNs and is useful for the synchronization study of MNNs.

The cluster output synchronization problem will be investigated in this article. Thus, the cluster output form of the system (5) is given by

$$\begin{cases} \dot{\tilde{x}}_\ell(t) = -S_\ell \tilde{x}_\ell(t) + \sum_{J=1}^{q} \Psi_{\ell J} \tilde{f}_J(\tilde{x}_J(t)) + \sum_{J=1}^{q} \Phi_{\ell J} \tilde{g}_J(\tilde{x}_J(t-\varepsilon_J(t))) + \tilde{\partial}_\ell^x(t) + \tilde{I}_\ell, \\ X_\ell^o(t) = W_\ell \tilde{x}_\ell(t), \quad \ell = 1,...,q \end{cases} \tag{7}$$

where $X_\ell^o(t)$ denotes the output of ℓth cluster in the drive system, $W_\ell = (w_{Z_{\ell-1}+1}, w_{Z_{\ell-1}+2}, ..., w_{Z_\ell})$ is the output weight vector, and other notations are $\tilde{x}_\ell(t) = (x_{Z_{\ell-1}+1}, x_{Z_{\ell-1}+2}, ..., x_{Z_\ell})^T$, $S_\ell = \text{diag}(s_{Z_{\ell-1}+1}, s_{Z_{\ell-1}+2}, ..., s_{Z_\ell})$, $\Psi_{\ell J} = (\psi_{ij})_{N_\ell \times N_J}$, $\Phi_{\ell J} = (\phi_{ij})_{N_\ell \times N_J}$, $\tilde{f}_J(\tilde{x}_J(t)) = (f_J(x_{Z_{J-1}+1}(t)), ..., f_J(x_{Z_J}(t)))^T$, $\tilde{g}_J(\tilde{x}_J(t-\varepsilon_J(t))) = (g_J(x_{Z_{J-1}+1}(t-\varepsilon_J(t))), ..., g_J(x_{Z_J}(t-\varepsilon_J(t))))^T$, $\tilde{\partial}_\ell^x(t) = (\partial_{Z_{\ell-1}+1}^x(t), ..., \partial_{Z_\ell}^x(t))^T$, $\tilde{I}_\ell(t) = (I_{Z_{\ell-1}+1}, ..., I_{Z_\ell})^T$.

Similarly, the cluster output form of the system (6) can be written as

$$\begin{cases} \dot{\tilde{y}}_\ell(t) = -S_\ell \tilde{y}_\ell(t) + \sum_{J=1}^{q} \Psi_{\ell J} \tilde{f}_J(\tilde{y}_J(t)) + \sum_{J=1}^{q} \Phi_{\ell J} \tilde{g}_J(\tilde{y}_J(t-\varepsilon_J(t))) + \tilde{\partial}_\ell^y(t) + U_\ell + \tilde{I}_\ell, \\ Y_\ell^o(t) = W_\ell \tilde{y}_\ell(t), \quad \ell = 1,...,q \end{cases} \tag{8}$$

where $Y_\ell^o(t)$ is the output of ℓth cluster in the response system, and other notations are defined similarly to those in (7).

Remark 2: Clustered behavior of neuron nodes is crucial for proper NNs functions [41]. In recent years, the cluster synchronization of traditional NNs have been extensively investigated [26–29]. Compared with traditional NNs, MNNs can better simulate actual NNs and have wider applicability [3]. Unfortunately, no research on cluster synchronization of MNNs has been reported. The main difficulty is that MNNs are a type of discontinuous state-dependent switching system, which can be treated as the model of traditional NNs with uncertain and mismatched coefficients. Therefore, cluster synchronization with respect to MNNs is more difficult to handle. By building the aforementioned model relationship, some handling techniques utilized in traditional NNs are referable for our study, and the problem is addressed with relative ease.

Before obtaining the main results, we introduce some useful assumptions, lemmas, and definitions.

Assumption (H_1): For any $z_1, z_2 \in \mathbb{R}$, there exist some constants $l_\ell > 0$, $l_\ell^* > 0$ and $d_\ell > 0$ $(\ell = 1, ..., q)$, such that activation functions $f_\ell(\cdot)$ and $g_\ell(\cdot)$ satisfy

$$|f_\ell(\cdot)| \le l_\ell,$$

$$|g_\ell(\cdot)| \le l_\ell^*,$$

$$|f_\ell(z_1) - f_\ell(z_2)| \le d_\ell |z_1 - z_2|.$$

Assumption (H_2): The time delay $\varepsilon_\ell(t)$ satisfies $0 < \varepsilon_\ell(t) \leq \varepsilon_\ell$ and $\dot{\varepsilon}_\ell(t) \leq \mu_\ell < 1$ ($\ell = 1, ..., q$), where $\mu_\ell > 0$, $\varepsilon_\ell > 0$ are some constants.

Lemma 1: The linear matrix inequality (LMI)

$$\chi = \begin{pmatrix} \chi_{11} & \chi_{12} \\ \chi_{21} & \chi_{22} \end{pmatrix} < 0$$

is equivalent to any one of the following two conditions:

$$(\mathrm{L}_1)\chi_{11} < 0, \chi_{22} - \chi_{12}^T \chi_{11}{}^{-1} \chi_{12} < 0$$
$$(\mathrm{L}_2)\chi_{22} < 0, \chi_{11} - \chi_{12}^T \chi_{22}{}^{-1} \chi_{12} < 0$$

where $\chi_{11}^T = \chi_{11}$ and $\chi_{22}^T = \chi_{22}$.

Lemma 2: Given any vectors $q, p \in \mathbb{R}^n$, the following inequality holds.

$$2q^T p \leq q^T q + p^T p.$$

Definition 2: Drive-response systems (1) and (4) are said to realize cluster output synchronization if for any initial values of the systems, the following equation holds

$$\lim_{t \to \infty} \left| Y_\ell^o(t) - X_\ell^o(t) \right| = 0$$

for $\ell = 1, 2, ..., q$.

Remark 3: Output synchronization for complex networks has been previously studied [42–44]; system output can be described as $Z(t) = Hx(t)$, where H denotes the output matrix. The system output forms indicate similarities in combining node states via a matrix or vector. However, our study is distinguishing from theirs. First, the dissipation coupling assumption condition (i.e., the sum of each row of coupling configuration matrix is 0), which is crucial for the synchronization of complex networks, had to be satisfied in these studies. However, this condition is strict for MNNs and does not need to be satisfied. Thus, the derived results from these studies are inapplicable to this study. Moreover, unlike general dynamic systems [42–44], MNNs, as a class of more complicated state-dependent switching dynamic systems, are taken into account in this study, which results in more complexity.

3. Main result

In this section, two control schemes are designed for the proposed synchronization model. In the first one, a feedback controller is designed for each cluster to reduce control costs. In the second one, multiple adjustable adaptive controllers are designed for each cluster, which can increase the anti-interference capacity of control system. In practical applications, two schemes can be flexibly chosen according to specific needs. Then, utilizing the control schemes and Lyapunov stability theory, some sufficient conditions are derived to ensure cluster output synchronization.

The system error is defined as $\tilde{\sigma}_\ell(t) = \tilde{y}_\ell(t) - \tilde{x}_\ell(t)$, and subtracting (7) from (8) yields the following error system:

$$\begin{cases} \dot{\tilde{\sigma}}_\ell(t) = -S_\ell \tilde{\sigma}_\ell(t) + \sum\limits_{J=1}^{q} \Psi_{\ell J} \hat{f}_J(\tilde{\sigma}_J(t)) + \sum\limits_{J=1}^{q} \Phi_{\ell J} \hat{g}_J(\tilde{\sigma}_J(t - \varepsilon_J(t))) + \tilde{\Pi}_\ell(t) + U_\ell, \\ \sigma_\ell^o(t) = W_\ell \tilde{\sigma}_\ell(t), \quad \ell = 1, ..., q \end{cases} \tag{9}$$

where $\hat{f}_J(\tilde{\sigma}_J(t)) = \tilde{f}_J(\tilde{x}_j(t)) - \tilde{f}_J(\tilde{y}_j(t))$, $\hat{g}_J(\tilde{e}_J(t - \varepsilon_J(t))) = \tilde{g}_J(\tilde{x}_J(t - \varepsilon_J(t))) - \tilde{g}_J(\tilde{y}_J(t - \varepsilon_J(t)))$ and $\tilde{\Pi}_\ell(t) = \tilde{\partial}_\ell^y - \tilde{\partial}_\ell^x = (\Pi_{Z_{\ell-1}+1}(t), ..., \Pi_{Z_\ell}(t))^T$.

3.1. The first control scheme

For convenience of the later study, the following notations are introduced. Let $\chi_\ell = \sum\limits_{J=1}^{q} \frac{\delta_J}{\delta_\ell} c_{J\ell}^{*}{}^{\tau b_m}$, $\upsilon_\ell = \rho + \sum\limits_{J=1}^{q} \sum\limits_{m=1}^{\tau-1} (c_{\ell J}{}^{\tau a_m} + c_{\ell J}^{*}{}^{\tau b_m}) + \frac{\chi_\ell e^{\rho\varepsilon}}{1-\mu_\ell}$, $o_\ell = \frac{\delta_J}{\delta_\ell} e^{\rho\varepsilon} \sum\limits_{J=1}^{q} c_{J\ell}{}^{\tau a_\tau}$, $\Upsilon_\ell = 2 \sum\limits_{i=1}^{N_\ell} \left| w_{z_{\ell-1}+i} \right| \sum\limits_{j=1}^{Z_q} \left(l_\ell \Delta\psi_{z_{\ell-1}+i,j} + l_\ell^* \Delta\phi_{z_{\ell-1}+i,j} \right)$, where $\delta_\ell, c_{\ell J}, c_{\ell J}^*, \rho$ are some positive constants, $\tau \geq 2$ is a integer, a_m and b_m are nonnegative constants and satisfy $\sum\limits_{m=1}^{\tau} a_m = \sum\limits_{m=1}^{\tau} b_m = 1$.

In this scheme, one controller is designed for each cluster. Without loss of generality, assume that the weight $w_{Z_{\ell-1}+1}$ of the first node $Z_{\ell-1}+1$ in the cluster ν_ℓ ($\ell = 1,2,...,q$) is not zero. Then, the controller is added to the first node and designed as follows

$$\begin{cases} u_{Z_{\ell-1}+1}(t) = -\sum_{i=1}^{N_\ell} \frac{w_{Z_{\ell-1}+i}}{w_{Z_{\ell-1}+1}} \left(k_{Z_{\ell-1}+i}\sigma_{Z_{\ell-1}+i}(t) + \xi_{Z_{\ell-1}+i}\text{sign}(W_\ell\tilde{\sigma}_\ell(t))\right), \\ u_{Z_{\ell-1}+j}(t) = 0, \quad j = 2,3,...,N_\ell \end{cases} \tag{10}$$

where $k_{Z_{\ell-1}+i}$ and $\xi_{Z_{\ell-1}+i}$ are control gains to be decided, sign$(\cdot)$ stands for standard sign function.

Note that by a simple calculation, it can be derived from (10) that

$$W_\ell U_\ell = -W_\ell K_\ell \tilde{\sigma}_\ell(t) - W_\ell \Gamma_\ell \text{Sgn}(W_\ell\tilde{\sigma}_\ell(t)) \tag{11}$$

where $W_\ell = (w_{z_{\ell-1}+1}, w_{z_{\ell-1}+2}, ..., w_{z_\ell})$, $U_\ell = (u_{z_{\ell-1}+1}, u_{z_{\ell-1}+2}, ..., u_{z_\ell})^T$, $K_\ell = \text{diag}(k_{Z_{\ell-1}+1}, k_{Z_{\ell-1}+2}, ..., k_{Z_\ell})$, $\Gamma_\ell = \text{diag}\,(\xi_{Z_{\ell-1}+1}, \xi_{Z_{\ell-1}+2}, ..., \xi_{Z_\ell})$ and $\text{Sgn}(W_\ell\tilde{\sigma}_\ell(t)) = \text{sign}(W_\ell\tilde{\sigma}_\ell(t)) \cdot 1_q$.

Theorem 1: Under Assumptions (H_1) and (H_2), drive system (1) and response system (4) can realize cluster output synchronization via the control scheme (10), if for some positive constants $\upsilon_\ell, o_\ell, M_{\ell J}, M^*_{\ell J}$ and Υ_ℓ ($\ell, J = 1,2,...,q$), the control parameters K_ℓ and Γ_ℓ meet the conditions *C1)* and *C2)*.

C1): $K_\ell + S_\ell = h_\ell I_{N_\ell}$, where h_ℓ meets $h_\ell \geq \frac{1}{\tau}(\upsilon_\ell + o_\ell)$, $\tau \geq 2$ is a known integer.

C2): $W_\ell\Gamma_\ell 1_\ell \geq \Upsilon_\ell + \sum_{J=1}^{q}(M_{\ell J} + M^*_{\ell J})$.

Proof: Construct the following Lyapunov-Krasovskii function:

$$V(t) = \sum_{\ell=1}^{q} \delta_\ell e^{\rho t}|W_\ell\tilde{\sigma}_\ell(t)|^\tau + \frac{e^{\rho\varepsilon}}{1-\mu_\ell}\sum_{\ell=1}^{q}\chi_\ell \int_{t-\varepsilon_\ell(t)}^{t} \Lambda_\ell(a)da$$

in which $\Lambda_\ell(a) = \delta_\ell e^{\rho\varepsilon_\ell}|W_\ell\tilde{\sigma}_\ell(a)|^\tau, a \geq 0$. Other notations used in this proof have been defined in the above.

Taking the upper right derivative of $V(t)$ along the error system obtains

$$\begin{aligned} D^+V(t) =& \sum_{\ell=1}^{q}\Big[\rho\delta_\ell e^{\rho t}|W_\ell\tilde{\sigma}_\ell(t)|^\tau + \tau\delta_\ell e^{\rho t}\ |W_\ell\tilde{\sigma}_\ell(t)|^{\tau-1}\text{sign}(W_\ell\tilde{\sigma}_\ell(t))W_\ell D^+\tilde{\sigma}_\ell(t)\Big] \\ &+ \frac{\chi_\ell e^{\rho\varepsilon}}{1-\mu_\ell}\sum_{\ell=1}^{q}[\Lambda_\ell(t) - (1-\dot{\varepsilon}_\ell(t))\Lambda_\ell(t-\varepsilon_\ell(t))] \\ \leq& \sum_{\ell=1}^{q}\Big[\rho\Lambda_\ell(t) + \tau\delta_\ell e^{\rho t}|W_\ell\tilde{\sigma}_\ell(t)|^{\tau-2}W_\ell\tilde{\sigma}_\ell(t)W_\ell\ D^+\tilde{\sigma}_\ell(t)\Big] \\ &+ \chi_\ell e^{\rho\varepsilon}\sum_{\ell=1}^{q}\Big[\frac{\Lambda_\ell(t)}{1-\mu_\ell} - \Lambda_\ell(t-\varepsilon_\ell(t))\Big] \end{aligned} \tag{12}$$

where Assumption (H_2) has been utilized.

First, we handle the second term in (12): $\tau\delta_\ell e^{\rho t}|W_\ell\tilde{\sigma}_\ell(t)|^{\tau-2}W_\ell\tilde{\sigma}_\ell(t)W_\ell D^+\tilde{\sigma}_\ell(t)$.

From (11), one can obtain

$$\begin{aligned} &\tau\delta_\ell e^{\rho t}|W_\ell\tilde{\sigma}_\ell(t)|^{\tau-2}W_\ell\tilde{\sigma}_\ell(t)W_\ell D^+\tilde{\sigma}_\ell(t) \\ =&\tau\delta_\ell e^{\rho t}|W_\ell\tilde{\sigma}_\ell(t)|^{\tau-2}W_\ell\tilde{\sigma}_\ell(t)W_\ell\Big[-S_\ell\tilde{\sigma}_\ell(t) + \sum_{J=1}^{q}\Psi_{\ell J}\hat{f}_J(\tilde{\sigma}_J(t)) \\ &+ \sum_{J=1}^{q}\Phi_{\ell J}\hat{g}_J(\tilde{\sigma}_J(t-\varepsilon_\ell(t))) + \tilde{\Pi}_\ell(t) - K_\ell\tilde{\sigma}_\ell(t) - \Gamma_\ell\text{Sgn}(W_\ell\tilde{\sigma}_\ell(t))\Big] \end{aligned} \tag{13}$$

Based on Assumption (H_1), one has

$$\begin{aligned} W_\ell\tilde{\sigma}_\ell(t)W_\ell\Psi_{\ell J}\hat{f}_J(\tilde{\sigma}_J(t)) &\le 2l_J\,|W_\ell\tilde{\sigma}_\ell(t)|\left|W_\ell\Psi_{\ell J}1_{N_J}\right| \\ &\le 2l_J\,|W_\ell\tilde{\sigma}_\ell(t)|\left|\sum_{m=1}^{N_J}\sum_{n=1}^{N_\ell} w_n\psi_{nm}\right|. \end{aligned}$$

Note that $2l_J\left|\sum_{m=1}^{N_J}\sum_{n=1}^{N_\ell} w_n\psi_{nm}\right|$ is a limited constant, and thus there exist some positive constants $M_{\ell J}$ and $\hat{c}_{\ell J}$ such that $2l_J\left|\sum_{m=1}^{N_J}\sum_{n=1}^{N_\ell} w_n\psi_{nm}\right| \le M_{\ell J} + \hat{c}_{\ell J}\,|W_J\tilde{\sigma}_J(t)|$, and note that $\hat{c}_{\ell J}\,|W_J\tilde{\sigma}_J(t)| \le c_{\ell J}\,|W_J\tilde{\sigma}_J(t)|$ where $c_{\ell J} = \max(\hat{c}_{\ell J}, \hat{c}_{J\ell})$.

Thus, we have

$$W_\ell\tilde{\sigma}_\ell(t)W_\ell\Psi_{\ell J}\hat{f}_J(\tilde{\sigma}_J(t)) \le M_{\ell J}\,|W_\ell\tilde{\sigma}_\ell(t)| + c_{\ell J}\,|W_\ell\tilde{\sigma}_\ell(t)|\,|W_J\tilde{\sigma}_J(t)|\,. \tag{14}$$

Similarly, based on Assumption (H_1), there exist positive constants $M^*_{\ell J}$ and $c^*_{\ell J}$ such that

$$\begin{aligned} W_\ell\tilde{\sigma}_\ell(t)W_\ell\Phi_{\ell J}\hat{g}_J(\tilde{\sigma}_J(t-\varepsilon_\ell(t))) &\le 2l^*_J\,|W_\ell\tilde{\sigma}_\ell(t)|\left|W_\ell\Phi_{\ell J}1_{N_J}\right| \\ &\le |W_\ell\tilde{\sigma}_\ell(t)|\,(M^*_{\ell J} + c^*_{\ell J}\,|W_J\tilde{\sigma}_J(t-\varepsilon_\ell(t))|) \\ &\le M^*_{\ell J}\,|W_\ell\tilde{\sigma}_\ell(t)| + c^*_{\ell J}\,|W_\ell\tilde{\sigma}_\ell(t)|\,|W_J\tilde{\sigma}_J(t-\varepsilon_J(t))| \end{aligned} \tag{15}$$

Substituting (14) and (15) into (13) yields

$$\begin{aligned} &\tau\delta_\ell e^{\rho t}|W_\ell\tilde{\sigma}_\ell(t)|^{\tau-2}W_\ell\tilde{\sigma}_\ell(t)W_\ell D^+\tilde{\sigma}_\ell(t) \\ &\le \tau\delta_\ell e^{\rho t}|W_\ell\tilde{\sigma}_\ell(t)|^{\tau-2}\Big\{W_\ell\tilde{\sigma}_\ell(t)W_\ell\Big[(-S_\ell - K_\ell)\tilde{\sigma}_\ell(t) + \tilde{\Pi}_\ell(t) - \Gamma_\ell\mathrm{Sgn}(W_\ell\tilde{\sigma}_\ell(t))\Big] \\ &+ \sum_{J=1}^{q} c_{\ell J}\,|W_\ell\tilde{\sigma}_\ell(t)|\,|W_J\tilde{\sigma}_J(t)| + \sum_{J=1}^{q} c^*_{\ell J}\,|W_\ell\tilde{\sigma}_\ell(t)|\,|W_J\tilde{\sigma}_J(t-\varepsilon_J(t))| + \sum_{J=1}^{q}(M_{\ell J} + M^*_{\ell J})\,|W_\ell\tilde{\sigma}_\ell(t)|\Big\} \end{aligned}$$

Based on Assumption (H_1), it is derived that

$$\begin{aligned} W_\ell\tilde{\Pi}_\ell(t) &= \sum_{i=1}^{N_\ell} w_{z_{\ell-1}+i}\Pi_{z_{\ell-1}+i}(t) \\ &\le \sum_{i=1}^{N_\ell}\left|w_{z_{\ell-1}+i}\right|\left(\left|\partial^y_{z_{\ell-1}+i}(t)\right| + \left|\partial^x_{z_{\ell-1}+i}(t)\right|\right) \\ &\le 2\sum_{i=1}^{N_\ell}\left|w_{z_{\ell-1}+i}\right|\sum_{j=1}^{Z_q}(l_\ell\Delta\psi_{z_{\ell-1}+i,j} + l^*_\ell\Delta\phi_{z_{\ell-1}+i,j}) \end{aligned}$$

and let

$$\Upsilon_\ell \triangleq 2\sum_{i=1}^{N_\ell}\left|w_{z_{\ell-1}+i}\right|\sum_{j=1}^{Z_q}(l_\ell\Delta\psi_{z_{\ell-1}+i,j} + l^*_\ell\Delta\phi_{z_{\ell-1}+i,j}) \tag{16}$$

Then, we have

$$W_\ell\tilde{\sigma}_\ell(t)W_\ell(-\Gamma_\ell\mathrm{Sgn}(W_\ell\tilde{\sigma}_\ell(t)) + \tilde{\Pi}_\ell(t)) \le (-W_\ell\Gamma_\ell 1_\ell + \Upsilon_\ell)\,|W_\ell\tilde{\sigma}_\ell(t)|$$

Thus, it is followed that

$$\begin{aligned} &\tau\delta_\ell e^{\rho t}|W_\ell\tilde{\sigma}_\ell(t)|^{\tau-2}W_\ell\tilde{\sigma}_\ell(t)W_\ell D^+\tilde{\sigma}_\ell(t) \\ &\le \tau\delta_\ell e^{\rho t}|W_\ell\tilde{\sigma}_\ell(t)|^{\tau-2}\Big\{W_\ell\tilde{\sigma}_\ell(t)W_\ell(-S_\ell - K_\ell)\tilde{\sigma}_\ell(t) + \sum_{J=1}^{q} c_{\ell J}\,|W_\ell\tilde{\sigma}_\ell(t)|\,|W_J\tilde{\sigma}_J(t)| \\ &+ \sum_{J=1}^{q} c^*_{\ell J}\,|W_\ell\tilde{\sigma}_\ell(t)|\,|W_J\tilde{\sigma}_J(t-\varepsilon_J(t))| - [W_\ell\Gamma_\ell 1_\ell - \Upsilon_\ell - \sum_{J=1}^{q}(M_{\ell J} + M^*_{\ell J})]\,|W_\ell\tilde{\sigma}_\ell(t)|\Big\} \end{aligned}$$

From the condition *C1)* and *C2)*, one has

$$\sum_{\ell=1}^{q}[W_\ell\Gamma_\ell 1_\ell - \Upsilon_\ell - \sum_{J=1}^{q}(M_{\ell J}+M^*_{\ell J})]\left|(W_\ell\tilde{\sigma}_\ell(t))^T\right| \le 0$$

and

$$W_\ell\tilde{\sigma}_\ell(t)W_\ell(-S_\ell - K_\ell)\tilde{\sigma}_\ell(t) = -h_\ell W_\ell\tilde{\sigma}_\ell(t)W_\ell\tilde{\sigma}_\ell(t)$$

Therefore, we obtain

$$\begin{aligned}
&\tau\delta_\ell e^{\rho t}|W_\ell\tilde{\sigma}_\ell(t)|^{\tau-2}W_\ell\tilde{\sigma}_\ell(t)W_\ell D^+\tilde{\sigma}_\ell(t)\\
&\quad\le -\tau h_\ell\delta_\ell e^{\rho t}|W_\ell\tilde{\sigma}_\ell(t)|^\tau + \delta_\ell e^{\rho t}\sum_{J=1}^{q}\tau c_{\ell J}|W_\ell\tilde{\sigma}_\ell(t)|^{\tau-1}\,|W_J\tilde{\sigma}_J(t)|\\
&\qquad + \delta_\ell e^{\rho t}\sum_{J=1}^{q}\tau c^*_{\ell J}|W_\ell\tilde{\sigma}_\ell(t)|^{\tau-1}\,|W_J\tilde{\sigma}_J(t-\varepsilon_J(t))|
\end{aligned} \tag{17}$$

According to the fact

$$\tau s_1 s_2\cdots s_\tau \le s_1^\tau + s_1^\tau + \cdots + s_\tau^\tau,\ s_i\ge 0,\ i=1,2,\cdots,\tau$$

it can be deduced that

$$\begin{aligned}
&\delta_\ell e^{\rho t}\sum_{J=1}^{q}\tau c_{\ell J}|W_\ell\tilde{\sigma}_\ell(t)|^{\tau-1}\,|W_J\tilde{\sigma}_J(t)|\\
&= \delta_\ell e^{\rho t}\sum_{J=1}^{q}\tau\left[\prod_{m=1}^{\tau-1}{c_{\ell J}}^{a_m}\,|W_\ell\tilde{\sigma}_\ell(t)|\right]{c_{\ell J}}^{a_\tau}\,|W_J\tilde{\sigma}_J(t)|\\
&\le \delta_\ell e^{\rho t}\sum_{J=1}^{q}\sum_{m=1}^{\tau-1}{c_{\ell J}}^{\tau a_m}|W_\ell\tilde{\sigma}_\ell(t)|^\tau + \delta_\ell e^{\rho t}\sum_{J=1}^{q}{c_{\ell J}}^{\tau a_\tau}|W_J\tilde{\sigma}_J(t)|^\tau
\end{aligned} \tag{18}$$

and

$$\begin{aligned}
&\delta_\ell e^{\rho t}\sum_{J=1}^{q}\tau c^*_{\ell J}|W_\ell\tilde{\sigma}_\ell(t)|^{\tau-1}\,|W_J\tilde{\sigma}_J(t-\varepsilon_J(t))|\\
&= \delta_\ell e^{\rho t}\sum_{J=1}^{q}\tau\left[\prod_{m=1}^{\tau-1}{c^*_{\ell J}}^{b_m}\,|W_\ell\tilde{\sigma}_\ell(t)|\right]{c^*_{\ell J}}^{b_\tau}\,|W_J\tilde{\sigma}_J(t-\varepsilon_J(t))|\\
&\le \delta_\ell e^{\rho t}\sum_{J=1}^{q}\sum_{m=1}^{\tau-1}{c^*_{\ell J}}^{\tau b_m}|W_\ell\tilde{\sigma}_\ell(t)|^\tau + \delta_\ell e^{\rho t}\sum_{J=1}^{q}{c^*_{\ell J}}^{\tau b_\tau}|W_J\tilde{\sigma}_J(t-\varepsilon_J(t))|^\tau
\end{aligned} \tag{19}$$

In light of (12), (17)-(19), we have

$$
\begin{aligned}
D^+V(t) \le & \sum_{\ell=1}^{q}\Big[\rho\Lambda_\ell(t) - \tau h_\ell\delta_\ell e^{\rho t}|W_\ell\tilde{\sigma}_\ell(t)|^\tau + \delta_\ell e^{\rho t}\sum_{J=1}^{q}\sum_{m=1}^{\tau-1} c_{\ell J}{}^{\tau a_m}|W_\ell\tilde{\sigma}_\ell(t)|^\tau \\
& + \delta_\ell e^{\rho t}\sum_{J=1}^{q} c_{\ell J}{}^{\tau a_\tau}|W_J\tilde{\sigma}_J(t)|^\tau + \delta_\ell e^{\rho t}\sum_{J=1}^{q}\sum_{m=1}^{\tau-1} c_{\ell J}^{*}{}^{\tau b_m}|W_\ell\tilde{\sigma}_\ell(t)|^\tau \\
& + \delta_\ell e^{\rho t}\sum_{J=1}^{q} c_{\ell J}^{*}{}^{\tau b_\tau}|W_J\tilde{\sigma}_J(t-\varepsilon_J(t))|^\tau\Big] + \chi_\ell e^{\rho\varepsilon}\sum_{\ell=1}^{q}\big[\frac{\Lambda_\ell(t)}{1-\mu_\ell} - \Lambda_\ell(t-\varepsilon_\ell(t))\big] \\
\le & \sum_{\ell=1}^{q}\Big[(-\tau h_\ell + \rho + \sum_{J=1}^{q}\sum_{m=1}^{\tau-1} c_{\ell J}{}^{\tau a_m} + \sum_{J=1}^{q}\sum_{m=1}^{\tau-1} c_{\ell J}^{*}{}^{\tau b_m})\Lambda_\ell(t) + \frac{\delta_\ell}{\delta_J}\sum_{J=1}^{q} c_{\ell J}{}^{\tau a_\tau}\Lambda_J(t) \\
& + \frac{\delta_\ell}{\delta_J}e^{\rho\varepsilon}\sum_{J=1}^{q} c_{\ell J}^{*}{}^{\tau b_\tau}\Lambda_J(t-\varepsilon_J(t))\Big] + \chi_\ell e^{\rho\varepsilon}\sum_{\ell=1}^{q}\big[\frac{\Lambda_\ell(t)}{1-\mu_\ell} - \Lambda_\ell(t-\varepsilon_\ell(t))\big]
\end{aligned}
$$

Then, according to the definitions of χ_ℓ, υ_ℓ and o_ℓ and utilizing the condition *C1)*, it is derived that

$$
\begin{aligned}
D^+V(t) \le & \sum_{\ell=1}^{q}\Big[(-\tau h_\ell + \rho + \sum_{J=1}^{q}\sum_{m=1}^{\tau-1} c_{\ell J}{}^{\tau a_m} + \sum_{J=1}^{q}\sum_{m=1}^{\tau-1} c_{\ell J}^{*}{}^{\tau b_m} + \frac{\chi_\ell e^{\rho\varepsilon}}{1-\mu_\ell})\Lambda_\ell(t) + \frac{\delta_\ell}{\delta_J}e^{\rho\varepsilon}\sum_{J=1}^{q} c_{\ell J}{}^{\tau a_\tau}\Lambda_J(t)\Big] \\
= & -\sum_{\ell=1}^{q}(\tau h_\ell - \upsilon_\ell - o_\ell)\Lambda_\ell(t) \le 0
\end{aligned}
$$

Thus, we have $V(t) \le V(0)$ for all $t \ge 0$. According to the definition of $V(t)$, it is derived that $\sum_{\ell=1}^{q}\delta_\ell e^{\rho t}|W_\ell\tilde{\sigma}_\ell(t)|^\tau \le V(t)$. Since $V(0)$ is a limited constant, there exist some positive constants $\varpi_\ell, \ell = 1, ..., q$, such that $\delta_\ell e^{\rho t}|W_\ell\tilde{\sigma}_\ell(t)|^\tau \le \varpi_\ell{}^\tau \le V(0)$. Hence, $|W_\ell\tilde{\sigma}_\ell(t)| \le \delta_\ell{}^{-\frac{1}{\tau}}\varpi_\ell e^{-\frac{\rho}{\tau}t}, t \ge 0$.

According to Definition 2, drive system (1) and response system (4) realize cluster output synchronization under the control scheme (10). This completes the proof.

Remark 4: In this control scheme, one feedback controller is devised for each cluster, which helps to save control costs and is easily implemented in practice. However, this control scheme may be fragile if the sole controller in cluster is subjected to malicious attacks. Specifically, owing to many nodes existing in each cluster, multiple controllers can be designed and added to these nodes for output synchronization in each cluster. Thus, a more flexible control scheme can be designed.

3.2. The second control scheme

The first scheme uses feedback control, and the obtained control gains k_i and ξ_i $(i \in \nu_\ell, \ell = 1, \cdots, q)$ may be much larger than those practical applications need owing to algorithm conservativeness. Thus, adaptive control, as a method to reduce control gain effectively, is utilized in this scheme. Compared with the first one, it aims to reduce the control gains and increase the anti-interference capacity of the system by designing some adjustable controllers.

In the cluster ν_ℓ $(\ell = 1, \cdots, q)$, without loss of generality, the weights of the first o_ℓ nodes are assumed to be non-zero, where $o_\ell \le N_\ell$ is a positive integer. Then, the adaptive controllers are added to those nodes and designed as

$$
u_{Z_{\ell-1}+m}(t) = \begin{cases} \sum_{i=1}^{N_\ell}\frac{p_{mi}^{\ell}(t)w_{Z_{\ell-1}+i}}{w_{Z_{\ell-1}+m}}[-k_{Z_{\ell-1}+i}(t)\sigma_{Z_{\ell-1}+i}(t) - \xi_{Z_{\ell-1}+i}(t)\mathrm{sign}(W_\ell\tilde{\sigma}_\ell(t))], & m = 1, \ldots, o_\ell \\ 0, & m = o_\ell + 1, ..., N_\ell \end{cases} \tag{20}
$$

where $p_{mi}^{\ell}(t)$ denotes the switching control parameter and its value is 0 or 1, and the adaptive updating laws of $k_{Z_{\ell-1}+i}(t)$ and $\xi_{Z_{\ell-1}+i}(t)$ are designed as

$$
\begin{cases} \dot{k}_{Z_{\ell-1}+i}(t) = e^{\rho t}a_{Z_{\ell-1}+i}\sigma_{Z_{\ell-1}+i}(t)(W_\ell\tilde{\sigma}_\ell(t))^T \\ \dot{\xi}_{Z_{\ell-1}+i}(t) = e^{\rho t}b_{Z_{\ell-1}+i}|W_\ell\tilde{\sigma}_\ell(t)| \end{cases} \tag{21}
$$

where $a_{Z_{\ell-1}+i} > 0, b_{Z_{\ell-1}+i} > 0, \rho > 0$ are some known constants.

It is noted that when $p^{\ell}_{mi}(t)$ satisfies $\sum\limits_{m=1}^{O_\ell}\sum\limits_{i=1}^{N_\ell} p^{\ell}_{mi}(t) = N_\ell$, it can be calculated that

$$W_\ell U_\ell = -W_\ell K_\ell(t)\tilde{\sigma}_\ell(t) - W_\ell \Gamma_\ell(t)\mathrm{Sgn}(W_\ell\tilde{\sigma}_\ell(t)) \tag{22}$$

where $W_\ell = (w_{z_{\ell-1}+1}, w_{z_{\ell-1}+2}, ..., w_{z_\ell})$, $U_\ell = (u_{z_{\ell-1}+1}, u_{z_{\ell-1}+2}, ..., u_{z_\ell})^T$, $K_\ell(t) = \mathrm{diag}(k_{Z_{\ell-1}+1}(t), k_{Z_{\ell-1}+2}(t), ..., k_{Z_\ell}(t))$, $\Gamma_\ell(t) = \mathrm{diag}(\xi_{Z_{\ell-1}+1}(t), \xi_{Z_{\ell-1}+2}(t), ..., \xi_{Z_\ell}(t))$ and $\mathrm{Sgn}(W_\ell\tilde{\sigma}_\ell(t)) = \mathrm{sign}(W_\ell\tilde{\sigma}_\ell(t)) \cdot 1_q$.

Remark 5: In the existing literatures, controllers are usually unadjustable during synchronization. With respect to the characteristic of the proposed model, switching control parameters $p^{\ell}_{mi}(t)$ ($m = 1, ..., o_\ell$, $i = 1, ..., N_\ell$, $\ell = 1, ..., q$) are introduced in the scheme (20). It is seen from (20) that the position and the number of the controllers in the cluster ν_ℓ are adjustable by taking different values of $p^{\ell}_{mi}(t)$. For example, let $s_\ell \le o_\ell$ ($\ell = 1, ..., q$) be an arbitrary positive integer and take $\sum_{i=1}^{N_\ell} p^{\ell}_{mi}(t) = N_\ell$, $m = s_\ell$ and $\sum_{i=1}^{N_\ell} p^{\ell}_{mi}(t) = 0$, $m \ne s_\ell$ in (20). Then, one controller is obtained in the cluster ν_ℓ, and its position is variable depending on the value of s_ℓ. Also, multiple controllers can be obtained by the proper values of $p^{\ell}_{mi}(t)$. Importantly, $p^{\ell}_{mi}(t)$ is time-varying and thus the controllers can be adjusted in real time, which can be designed as the switch trigger in practical applications. Hence, if the systems are maliciously attacked, timely adjustment of the values of $p^{\ell}_{mi}(t)$ can help remedy sudden control problems. In the final simulations, an example will be given to verify the effectiveness of this control scheme.

Theorem 2: If Assumptions (H_1) and (H_2) are satisfied and the control parameter $p^{\ell}_{mi}(t)$ meets $\sum\limits_{m=1}^{O_\ell}\sum\limits_{i=1}^{N_\ell} p^{\ell}_{mi}(t) = N_\ell$ ($\ell = 1, ..., q$), drive system (1) and response system (4) can realize cluster output synchronization under the control scheme (20).

Proof: Construct the following Lyapunov-Krasovskii function:

$$V(t) = V_1(t) + V_2(t) + V_3(t) \tag{23}$$

$$V_1(t) = \sum_{\ell=1}^{q} \alpha e^{\rho t}(W_\ell\tilde{\sigma}_\ell(t))^T W_\ell\tilde{\sigma}_\ell(t)$$

$$V_2(t) = \alpha\sum_{\ell=1}^{q}\sum_{J=1}^{N_\ell}\Big[\frac{w_{Z_{\ell-1}+J}}{a_i}(k_{Z_{\ell-1}+J}(t) - \hat{k}_{Z_{\ell-1}+J})^2 + \frac{w_{Z_{\ell-1}+J}}{b_i}(\xi_{Z_{\ell-1}+J}(t) - \hat{\xi}_{Z_{\ell-1}+J})^2\Big]$$

$$V_3 = \sum_{\ell=1}^{q}\int_{t-\varepsilon_\ell(t)}^{t} e^{\rho(\varepsilon_\ell+s)}\vartheta_\ell(W_\ell\tilde{\sigma}_\ell(s))^T W_\ell\tilde{\sigma}_\ell(s)ds.$$

where $\alpha, \hat{\xi}_i, \hat{k}_i, \vartheta_i$ are some positive constants.

First, taking the derivative of $V_1(t)$ can obtain

$$\begin{aligned}\dot{V}_1(t) &= \sum_{\ell=1}^{q}\Big[2\alpha e^{\rho t}(W_\ell\tilde{\sigma}_\ell(t))^T W_\ell\dot{\tilde{\sigma}}_\ell(t) + \alpha\rho e^{\rho t}(W_\ell\tilde{\sigma}_\ell(t))^T W_\ell\tilde{\sigma}_\ell(t)\Big]\\ &= 2\alpha e^{\rho t}\sum_{\ell=1}^{q}(W_\ell\tilde{\sigma}_\ell(t))^T W_\ell\Big[-S_\ell\tilde{\sigma}_\ell(t) + \sum_{J=1}^{q}\Psi_{\ell J}\hat{f}_J(\tilde{\sigma}_J(t)) + \sum_{J=1}^{q}\Phi_{\ell J}\hat{g}_J(\tilde{\sigma}_J(t-\varepsilon_\ell(t)))\\ &\quad + \tilde{\Pi}_\ell(t) - K_\ell(t)\tilde{\sigma}_\ell(t) - \Gamma_\ell(t)\mathrm{Sgn}(W_\ell\tilde{\sigma}_\ell(t))\Big] + \alpha\rho e^{\rho t}\sum_{\ell=1}^{q}(W_\ell\tilde{\sigma}_\ell(t))^T W_\ell\tilde{\sigma}_\ell(t)\end{aligned} \tag{24}$$

Considering that

$$\begin{aligned}&2\alpha e^{\rho t}\sum_{\ell=1}^{q}(W_\ell\tilde{\sigma}_\ell(t))^T W_\ell[\tilde{\Pi}_\ell(t) - \Gamma_\ell(t)\mathrm{Sgn}(W_\ell\tilde{\sigma}_\ell(t))]\\ &\qquad \le 2\alpha e^{\rho t}\sum_{\ell=1}^{q}\sum_{J=1}^{N_\ell} w_{Z_{\ell-1}+J}(\big|\Pi_{Z_{\ell-1}+J}(t)\big| - \xi_{Z_{\ell-1}+J}(t))\,|W_\ell\tilde{\sigma}_\ell(t)|,\end{aligned}$$

and by employing (14) and (15), we obtain

$$
\begin{aligned}
\dot{V}_1(t) \leq{} & 2\alpha e^{\rho t} \sum_{\ell=1}^{q} (W_\ell \tilde{\sigma}_\ell(t))^T W_\ell(-S_\ell - K_\ell(t))_\ell \tilde{\sigma}_\ell(t) + 2\alpha e^{\rho t} \sum_{\ell=1}^{q} \sum_{J=1}^{N_\ell} w_{Z_{\ell-1}+J}(\Pi_{Z_{\ell-1}+J}(t) - \xi_{Z_{\ell-1}+J}(t)) \, |W_\ell \tilde{\sigma}_\ell(t)| \\
& + 2\alpha e^{\rho t} \sum_{\ell=1}^{q} \sum_{J=1}^{q} (M_{\ell J} + M^*_{\ell J}) \left|(W_\ell \tilde{e}_\ell(t))^T\right| + 2\alpha e^{\rho t} \sum_{\ell=1}^{q} \sum_{J=1}^{q} c_{\ell J} \left|(W_\ell \tilde{e}_\ell(t))^T\right| |W_J \tilde{\sigma}_J(t)| \\
& + 2\alpha e^{\rho t} \sum_{\ell=1}^{q} \sum_{J=1}^{q} c^*_{\ell J} \left|(W_\ell \tilde{\sigma}_\ell(t))^T\right| |W_J \tilde{\sigma}_J(t - \varepsilon_\ell(t))| + \alpha \rho e^{\rho t} \sum_{\ell=1}^{q} (W_\ell \tilde{\sigma}_\ell(t))^T W_\ell \tilde{\sigma}_\ell(t)
\end{aligned}
$$

According to the adaptive law (21), computing the derivative of $V_2(t)$ gets

$$
\begin{aligned}
\dot{V}_2(t) ={} & 2\alpha \sum_{\ell=1}^{q} \sum_{J=1}^{N_\ell} w_{Z_{\ell-1}+J}(k_{Z_{\ell-1}+J}(t) - \hat{k}_{Z_{\ell-1}+J}) \sigma_{Z_{\ell-1}+J}(t) e^{\rho t} (W_\ell \tilde{\sigma}_\ell(t))^T \\
& + 2\alpha \sum_{\ell=1}^{q} \sum_{J=1}^{N_\ell} w_{Z_{\ell-1}+J}(\xi_{Z_{\ell-1}+J}(t) - \hat{\xi}_{Z_{\ell-1}+J}) e^{\rho t} \, |W_\ell \tilde{\sigma}_\ell(t)| \\
={} & 2\alpha e^{\rho t} \sum_{\ell=1}^{q} (W_\ell \tilde{\sigma}_\ell(t))^T W_\ell (K_\ell(t) - \hat{K}_\ell) \tilde{\sigma}_\ell(t) \\
& + 2\alpha e^{\rho t} \sum_{\ell=1}^{q} \sum_{J=1}^{N_\ell} w_{Z_{\ell-1}+J}(\xi_{Z_{\ell-1}+J}(t) - \hat{\xi}_{Z_{\ell-1}+J}) \, |W_\ell \tilde{\sigma}_\ell(t)|
\end{aligned}
\tag{25}
$$

Computing the derivative of $V_3(t)$ along the error system obtains

$$
\dot{V}_3(t) \leq \sum_{\ell=1}^{q} e^{\rho(\varepsilon_\ell + t)} \vartheta_\ell (W_\ell \tilde{\sigma}_\ell(t))^T W_\ell \tilde{\sigma}_\ell(t) - e^{\rho t} \sum_{\ell=1}^{q} (1 - \mu_\ell) \vartheta_\ell (W_\ell \tilde{\sigma}_\ell(t - \varepsilon_\ell(t)))^T W_\ell \tilde{\sigma}_\ell(t - \varepsilon_\ell(t)) \tag{26}
$$

where Assumption (H_2) has been utilized.
By (24), (25) and (26), one has

$$
\begin{aligned}
\dot{V}(t) \leq{} & 2\alpha e^{\rho t} \sum_{\ell=1}^{q} (W_\ell \tilde{\sigma}_\ell(t))^T W_\ell(-S_\ell - \hat{K}_\ell) \tilde{\sigma}_\ell(t) + 2\alpha e^{\rho t} \sum_{\ell=1}^{q} \sum_{J=1}^{N_\ell} w_{Z_{\ell-1}+J}(\left|\Pi_{Z_{\ell-1}+J}(t)\right| - \hat{\xi}_{Z_{\ell-1}+J}) \, |W_\ell \tilde{\sigma}_\ell(t)| \\
& + 2\alpha e^{\rho t} \sum_{\ell=1}^{q} (M_{\ell j} + M^*_{\ell j}) \left|(W_\ell \tilde{\sigma}_\ell(t))^T\right| + 2\alpha e^{\rho t} \sum_{\ell=1}^{q} \sum_{J=1}^{q} c_{\ell J} \left|(W_\ell \tilde{\sigma}_\ell(t))^T\right| |W_J \tilde{\sigma}_J(t)| \\
& + 2\alpha e^{\rho t} \sum_{\ell=1}^{q} \sum_{J=1}^{q} c^*_{\ell J} \left|(W_\ell \tilde{\sigma}_\ell(t))^T\right| |W_J \tilde{\sigma}_J(t - \varepsilon_J(t))| + \alpha \rho e^{\rho t} \sum_{\ell=1}^{q} (W_\ell \tilde{\sigma}_\ell(t))^T W_\ell \tilde{\sigma}_\ell(t) \\
& + e^{\rho t} \sum_{\ell=1}^{q} e^{\rho \varepsilon_\ell} \vartheta_\ell (W_\ell \tilde{\sigma}_\ell(t))^T W_\ell \tilde{\sigma}_\ell(t) - e^{\rho t} \sum_{\ell=1}^{q} (1 - \mu_\ell) \vartheta_\ell (W_\ell \tilde{\sigma}_\ell(t - \tau_\ell(t)))^T W_\ell \tilde{\sigma}_\ell(t - \varepsilon_\ell(t))
\end{aligned}
$$

Now, we tackle the second term : $2\alpha e^{\rho t} \sum\limits_{\ell=1}^{q} \sum\limits_{J=1}^{N_\ell} w_{Z_{\ell-1}+J}(\left|\Pi_{Z_{\ell-1}+J}(t)\right| - \hat{\xi}_{Z_{\ell-1}+J}) \, |W_\ell \tilde{\sigma}_\ell(t)|$. First, note that

$$
\left|\Pi_{z_{\ell-1}+J}(t)\right| \leq \left|\partial^y_{z_{\ell-1}+J}(t)\right| + \left|\partial^x_{z_{\ell-1}+J}(t)\right| \leq 2 \sum_{i=1}^{Z_q} (l_\ell \Delta\psi_{z_{\ell-1}+J,i} + l^*_\ell \Delta\phi_{z_{\ell-1}+J,i})
$$

Then, by taking $\hat{\xi}_{Z_{\ell-1}+J} = \hat{\xi}^*_{Z_{\ell-1}+J} + \hat{\xi}^{**}_{Z_{\ell-1}+J}$, where $\hat{\xi}^*_{Z_{\ell-1}+J} = 2 \sum\limits_{i=1}^{Z_q} (l_\ell \Delta\psi_{z_{\ell-1}+J,i} + l^*_\ell \Delta\phi_{z_{\ell-1}+J,i})$ and $\sum\limits_{J=1}^{N_\ell} \hat{\xi}^{**}_{Z_{\ell-1}+J} = M_{\ell J} + M^*_{\ell J}$, we have

$$2\alpha e^{\rho t}\sum_{\ell=1}^{q}\sum_{J=1}^{N_\ell} w_{z_{\ell-1}+J}(\left|\Pi_{z_{\ell-1}+J}(t)\right| - \hat{\xi}_{z_{\ell-1}+J})\,|W_\ell\tilde{\sigma}_\ell(t)| \le -2\alpha e^{\rho t}\sum_{\ell=1}^{q}(M_{\ell J}+M^*_{\ell J})\left|(W_\ell\tilde{\sigma}_\ell(t))^T\right|$$

Thus, one has

$$\begin{aligned}\dot{V}(t) \le\ & 2\alpha e^{\rho t}\sum_{\ell=1}^{q}(W_\ell\tilde{\sigma}_\ell(t))^T W_\ell(-S_\ell - \hat{K}_\ell)\tilde{\sigma}_\ell(t) + 2\alpha e^{\rho t}\sum_{\ell=1}^{q}\sum_{J=1}^{q} c_{\ell J}\left|(W_\ell\tilde{\sigma}_\ell(t))^T\right||W_J\tilde{\sigma}_J(t)| \\ & + 2\alpha e^{\rho t}\sum_{\ell=1}^{q}\sum_{J=1}^{q} c^*_{\ell J}\left|(W_\ell\tilde{\sigma}_\ell(t))^T\right||W_J\tilde{\sigma}_J(t-\varepsilon_\ell(t))| + e^{\rho t}\sum_{\ell=1}^{q}(\alpha\rho + e^{\rho\varepsilon_\ell}\vartheta_\ell)(W_\ell\tilde{\sigma}_\ell(t))^T W_\ell\tilde{\sigma}_\ell(t) \\ & - e^{\rho t}\sum_{\ell=1}^{q}(1-\mu_\ell)\vartheta_\ell(W_\ell\tilde{\sigma}_\ell(t-\varepsilon_\ell(t)))^T W_\ell\tilde{\sigma}_\ell(t-\varepsilon_\ell(t))\end{aligned}$$

Let $\hat{K}_\ell = d_\ell I_{N_\ell} - S_\ell$, where $d_\ell > 0$ is a constant to be decided, and one obtains

$$\begin{aligned}\dot{V}(t) \le\ & e^{\rho t}\sum_{\ell=1}^{q}(-2\alpha d_\ell + \alpha\rho + e^{\rho\varepsilon_\ell}\vartheta_\ell)(W_\ell\tilde{\sigma}_\ell(t))^T W_\ell\tilde{\sigma}_\ell(t) + 2\alpha e^{\rho t}\sum_{\ell=1}^{q}\sum_{J=1}^{q} c_{\ell J}\left|(W_\ell\tilde{\sigma}_\ell(t))^T\right||W_J\tilde{\sigma}_J(t)| \\ & + 2\alpha e^{\rho t}\sum_{\ell=1}^{q}\sum_{J=1}^{q} c^*_{\ell J}\left|(W_\ell\tilde{\sigma}_\ell(t))^T\right||W_J\tilde{\sigma}_J(t-\varepsilon_\ell(t))| - e^{\rho t}\sum_{\ell=1}^{q}(1-\mu_\ell)\vartheta_\ell(W_\ell\tilde{\sigma}_\ell(t-\varepsilon_\ell(t)))^T W_\ell\tilde{\sigma}_\ell(t-\varepsilon_\ell(t))\end{aligned}$$

Introduce the following notations : $\varphi_1 = (|W_1\tilde{\sigma}_1(t)|, |W_2\tilde{\sigma}_2(t)|, ..., \left|W_q\tilde{\sigma}_q(t)\right|)^T$, $\varphi_2 = (|W_1\tilde{\sigma}_1(t-\varepsilon_\ell(t))|, |W_2\tilde{\sigma}_2(t-\varepsilon_\ell(t))|, ..., \left|W_q\tilde{\sigma}_q(t-\varepsilon_\ell(t))\right|)^T$, $\varphi = (\varphi_1\ \varphi_2)^T$, $\Omega = \mathrm{diag}(-2\alpha d_1 + \alpha\rho + e^{\rho\varepsilon_1}\vartheta_1, ..., -2\alpha d_q + \alpha\rho + e^{\rho\varepsilon_q}\vartheta_q)$, $\Xi = \mathrm{diag}(\vartheta_1 - \vartheta_1\mu_1, ..., \vartheta_q - \vartheta_q\mu_q)$.

Then, we can obtain

$$\begin{aligned}\dot{V}(t) &\le e^{\rho t}[\varphi_1^T\Omega\varphi_1 + 2\alpha\varphi_1^T C\varphi_1 + 2\alpha\varphi_1^T C^*\varphi_2 - \varphi_2^T\Xi\Theta\varphi_2] \\ &= e^{\rho t}\varphi^T\Sigma\varphi\end{aligned}$$

where $\Sigma = \begin{pmatrix}\Omega + 2\alpha C & \alpha C^* \\ \alpha C^{*T} & -\Xi\end{pmatrix}$

Let $d_\ell > \frac{\alpha\rho + e^{\rho\tau}\vartheta_\ell + 2\alpha\lambda_{\max}(C)}{2\alpha}$, $\ell = 1, ..., q$, and it is inferred that

$$\Omega + 2\alpha C < 0 \tag{27}$$

Because C^* is norm-bounded, there exists a positive constant $\gamma(C^{*T}C^*)$ such that $\left\|C^{*T}C^*\right\| \le \gamma(C^{*T}C^*)$. Thus, taking $0 < \sqrt{\alpha} < \lambda_{\min}(-\Omega - 2\alpha C)\beta/\gamma(C^{*T}C^*)$, where $\beta = \min\{\vartheta_i(1-\mu_i), i = 1, ..., q\}$, one has

$$\Omega + 2\alpha C + \alpha^2 C^{*T}\Xi^{-1}C^* < 0. \tag{28}$$

By Lemma 1, the inequalities (27) and (28) imply that $\Sigma < 0$.

Thus, it is obtained that $V(t) \le V(0)$ for all $t \ge 0$. According to (23), one has $\sum_{\ell=1}^{q}\alpha e^{\rho t}(W_\ell\tilde{\sigma}_\ell(t))^T W_\ell\tilde{\sigma}_\ell(t) \le V(0)$. Thus, there exist some constants $\delta_\ell, \ell = 1, ..., q$, such that $\alpha e^{\rho t}(W_\ell\tilde{\sigma}_\ell(t))^T W_\ell\tilde{\sigma}_\ell(t) \le \delta_\ell^2 \le V(0)$. Hence, $|W_\ell\tilde{\sigma}_\ell(t)| \le \sqrt{\alpha}\delta_\ell e^{-\frac{\rho}{2}t}, t \ge 0$.

According to Definition 2, drive system (1) and response system (4) realize cluster output synchronization under the control scheme (20). This completes the proof.

Remark 6: Feedback and adaptive controls are used to realize the synchronization of MNNs in this article, and they are also effective for the synchronization of traditional NNs. In many existing studies such as [28, 29, 45], some simple linear feedback and adaptive controllers were considered: $u(t) = k\sigma(t)$ and $u^*(t) = k^*(t)\sigma(t)$. However, they cannot ensure the synchronization of MNNs due to parameter mismatches, as indicated in [18, 19]. It can be found from the proofs of Theorems 1 and 2 that the control terms $\xi\text{sign}(\cdot)$ and $\xi(t)\text{sign}(\cdot)$ in (10) and (20) play a crucial role in eliminating the synchronization errors of MNNs. Some studies on traditional NNs [46, 47] also considered the control terms $\xi\text{sign}(\cdot)$ and $\xi(t)\text{sign}(\cdot)$, and the differences between their controllers and ours lie in two aspects. On the one hand, for the proposed cluster output synchronization model, the controller design is specific and different, such as containing the information of output weights, which is vital for cluster output synchronization. On the other hand, the switching control parameters $p^{\ell}_{mi}(t)$ are introduced in the proposed synchronization model, as discussed in Remark 5. Therefore, compared with the existing controllers in traditional NNs, the proposed one is more flexible and has a better anti-interference capacity.

Remark 7: Computational complexity is significant for analyzing operation efficiency of controllers. It is seen from (10) that the computation burden of the first scheme mainly includes a set of scalar addition, multiplication, division and comparison. Specifically, the scheme (10) involves $3N_\ell - 2$ additions, $4N_\ell$ multiplications, 1 division and 1 comparison where N_ℓ denotes the number of nodes in cluster $\nu_\ell(\ell = 1, 2, \cdots, q)$. By transforming these basic operations into multiplications [48], computational complexity of the first scheme is approximately $7N_\ell + 9$ multiplications. Applying the Big O notation, computational complexity can be expressed as $O(N_\ell)$. It is observed from (20) and (21) that the second scheme involves not only the basic operations (i.e., addition, multiplication, division and comparison), but also differentiation. Thus, on the one hand, by transforming the basic operations into multiplications, (20) and (21) totally involve $o_\ell N_\ell + 10o_\ell + 12N_\ell - 1$ multiplications where $o_\ell \leq N_\ell$ denotes the number of the non-zero weights in cluster ν_ℓ. The corresponding computational complexity using the Big O notation is $O(o_\ell N_\ell)$. On the other hand, to handle the differentiation in (21), computational complexity is $O(sk^3N_\ell)$ when applying Runge-Kutta method [49], where k is the number of stages of generating implicit Runge-Kutta method and s is the number of steps. Therefore, the overall complexity for the second control scheme is $O(o_\ell N_\ell + sk^3N_\ell)$. It is clear that computation complexities of two schemes grow linearly as the variables increase except k.

Remark 8: The purpose of synchronization in NNs is to control the networks toward the expected states for certain functions (e.g., accurate information expression [13]). Thus, fruitful results have been presented with regard to MNNs synchronization, which include various synchronization models such as quasi-synchronization [15], lag synchronization [16], adaptive synchronization[50], asymptotic synchronization [21], and exponential synchronization [18]. However, their model structures are monotonous and focus on the one-cluster networks. In fact, NNs include multiple clusters where the nodes from the same cluster collaborate and work together via the combination behaviors such as the weighted sum of nodes states [33–35]. Therefore, this article proposes cluster output synchronization model for MNNs. Figs.1 and 2 indicate that the proposed model can be reduced to the node-to-node model if one node exists in each cluster. Thus, our study can corroborate previous results, such as those in [20, 50], as special cases.

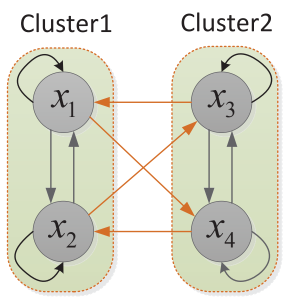

Figure 3: The network topology among four neuron nodes and the arrow represents the direction of information transfer.

4. Numerical simulation

In this section, we utilize several numerical simulations to verify the accuracy of the theoretical results.

Consider four-neuron MNNs (1) with the network topology shown in Fig. 3, where the nodes can be divided into two clusters, and the matrices of memristive connection coefficients in (2) and (3) are

$$\overleftarrow{\Psi} = (\overleftarrow{\psi}_{ij})_{4\times4} = \begin{bmatrix} -0.4 & 1.2 & 0.25 & 0 \\ 1.1 & -0.55 & 0 & 0.5 \\ 0 & 0.5 & -1.5 & 3 \\ 0.33 & 0 & 1 & -2 \end{bmatrix}$$

$$\vec{\Psi} = (\vec{\psi}_{ij})_{4\times4} = \begin{bmatrix} -0.5 & 1.3 & 0.26 & 0 \\ 1.2 & -0.45 & 0 & 0.45 \\ 0 & 0.51 & -1.2 & 2.4 \\ 0.32 & 0 & 0.8 & -1.6 \end{bmatrix}$$

$$\overleftarrow{\Phi} = (\overleftarrow{\phi}_{ij})_{4\times4} = \begin{bmatrix} -0.7 & 2.5 & 1.1 & 0 \\ 1.4 & -0.2 & 0 & 0.1 \\ 0 & 0.2 & -0.3 & 2.1 \\ 0.15 & 0 & 0.2 & -1.4 \end{bmatrix}$$

$$\vec{\Phi} = (\vec{\phi}_{ij})_{4\times4} = \begin{bmatrix} -0.9 & 2.1 & 1.12 & 0 \\ 1.3 & -0.3 & 0 & 0.12 \\ 0 & 0.14 & -0.33 & 2.4 \\ 0.1 & 0 & 0.22 & -1.6 \end{bmatrix}$$

In cluster 1, consider weight output vector $W_1 = (1\ 2)$, activation function $f_i(x) = g_i(x) = \sin(x)$, outside input $I_i = 0$, time-varying delay $\varepsilon_i(t) = e^t/(e^t+1)$, where $i = 1, 2$, self-inhibition $s_1 = 0.8$, $s_2 = 0.9$. In cluster 2, take $W_2 = (1\ 3)$, $f_i(x) = g_i(x) = \tanh(x)$, $I_i = 0$, $\varepsilon_i(t) = e^t/(2e^t+2)$, $i = 3, 4$, $s_1 = 1.2$, $s_2 = 1.1$. The initial value of the drive system (1) is considered as $x(t) = (-5, 7, -1, 2)^T$. The response system (4) whose initial value being set as $y(t) = (1, -1.3, 2, -1)^T$ has the same structure as the system (1).

It can be calculated from the above parameters that $\varepsilon_i(t) < \varepsilon_i = 1$, $\dot{\varepsilon}_i(t) < \mu_i = 0.5$, $l_i = l_i^* = 1$ $(i = 1, \ldots, 4)$, $M = (M_{ij})_{2\times2} = \begin{bmatrix} 4.2 & 2.41 \\ 2.96 & 2.7 \end{bmatrix}$, $M^* = (M^*_{ij})_{2\times2} = \begin{bmatrix} 7.4 & 2.66 \\ 1.09 & 3.87 \end{bmatrix}$, $\Upsilon_1 = 3.54$, $\Upsilon_2 = 7.88$. To guarantee the conditions in Theorem 1, one can take the control gains $K_1 = \begin{bmatrix} 3.9 & 0 \\ 0 & 3.8 \end{bmatrix}$, $K_2 = \begin{bmatrix} 4.0 & 0 \\ 0 & 4.1 \end{bmatrix}$ and $\xi_i = 7 (i = 1, ..., 4)$ in the feedback control scheme (10), and choose other parameters $\rho = 0.1$, $\tau = 2$, $a_i = b_i = 0.5$, $\delta_i = 1$, $i = 1, 2$. Then, it can be calculated that $h_1 = 4.7 > 0.5(\upsilon_1 + o_1) = 0.77$, $h_2 = 5.2 > 0.5(\upsilon_2 + o_2) = 0.62$, $w_1\xi_1 + w_2\xi_2 = 21 > \Upsilon_1 + \sum_{J=1}^{2}(M_{1J} + M^*_{1J}) = 20.2$ and $w_3\xi_3 + w_3\xi_3 = 28 > \Upsilon_2 + \sum_{J=1}^{2}(M_{2J} + M^*_{2J}) = 18.5$, which guarantees the conditions in Theorem 1.

Under the aforementioned settings, the node state trajectories in clusters 1 and 2 are depicted in Figs. 4 and 5, respectively. It is seen from the figures that the node $x_i(t)$ in the drive system is not synchronized with the node $y_i(t)$ $(i = 1, \cdots, 4)$ in the response system, which is confirmed by Fig. 6 where the node error signals do not tend to zero over time. In contrast, it can be observed from Fig. 7 that the combination outputs of error signals in each cluster quickly approach to zero, which validates the theoretical results of Theorem 1.

In the following, we will demonstrate the effectiveness of the adaptive control scheme (20).

Define switching control matrices $P^1(t) = (p^1_{ij}(t))_{2\times2}$ and $P^2(t) = (p^2_{ij}(t))_{2\times2}$, and take $P^1(t) = P^2(t) = \begin{pmatrix} 1 & 1 \\ 0 & 0 \end{pmatrix}$. In light of (20), we obtain two adaptive controllers u_1 and u_3 which are applied to clusters ν_1 and ν_2, respectively. Suppose that the adaptive control parameters in (21) are $(a_1\ a_2\ a_3\ a_4) = (0.15\ 0.2\ 0.25\ 0.3)$, $(b_1\ b_2\ b_3\ b_4) = (0.3\ 0.4\ 0.5\ 0.6)$, and $\rho = 0.05$. If the initial values in (21) are taken as $k_i(t) = 0.15$ and $\xi_i(t) = 0.5$ $(i = 1, ..., 4)$, the time responses of the node errors are presented in Fig. 8. It is seen from the figure that there is no synchronous behavior between the nodes. However, the simulation result of the combination outputs shown in Fig. 9 indicates that the systems realize cluster output synchronization. Meanwhile, the trajectories of the control gains k_i and ξ_i $(i = 1, ..., 4)$ are given in Figs. 10 and 11, respectively, which are obviously smaller than the obtained ones in the above scheme (10).

Next, to show the anti-interference capacity of the control scheme (20), we consider the case that the controllers u_1 and u_3 are attacked when $t = 1.5$s, that is, $u_1 = u_3 = 0$ for $t > 1.5$s. The simulation result is depicted in Fig. 12, where the error signals are increased from the attack instant. In order to handle this problem, one can adjust $P^1(t) = P^2(t) = \begin{pmatrix} 0 & 0 \\ 1 & 1 \end{pmatrix}$ at $t = 1.5$s and obtain two new controllers u_2 and u_4 which avoid the attacks to the original

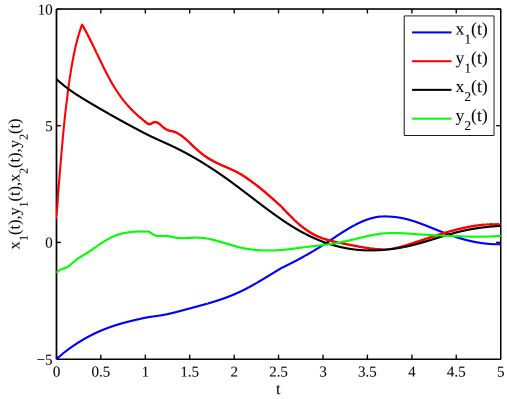

Figure 4: The node states of the drive and response systems in cluster 1 under the first control scheme.

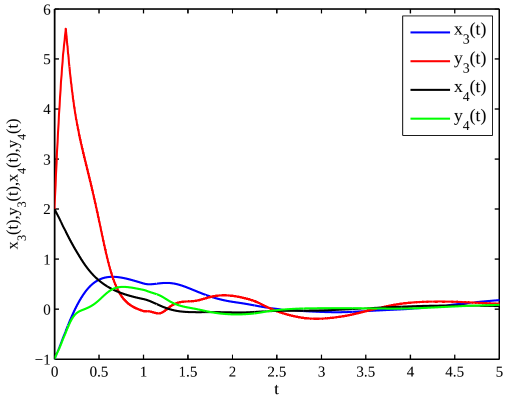

Figure 5: The node states of the drive and response systems in cluster 2 under the first control scheme.

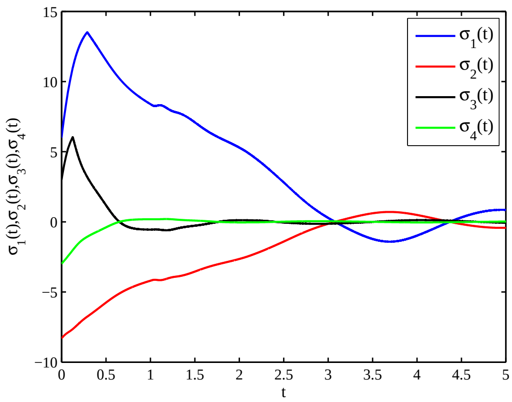

Figure 6: The node errors $\sigma_1(t)$, $\sigma_2(t)$, $\sigma_3(t)$ and $\sigma_4(t)$ under the first control scheme.

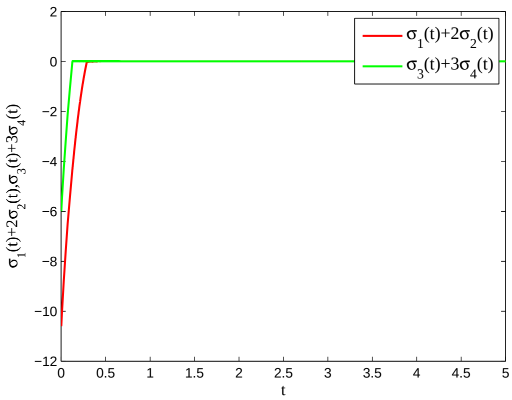

Figure 7: The combination outputs of error signals in clusters 1 and 2 under the first control scheme.

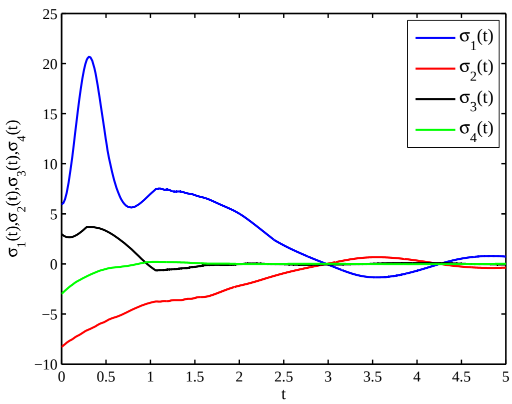

Figure 8: The node errors $\sigma_1(t)$, $\sigma_2(t)$, $\sigma_3(t)$ and $\sigma_4(t)$ under the second control scheme.

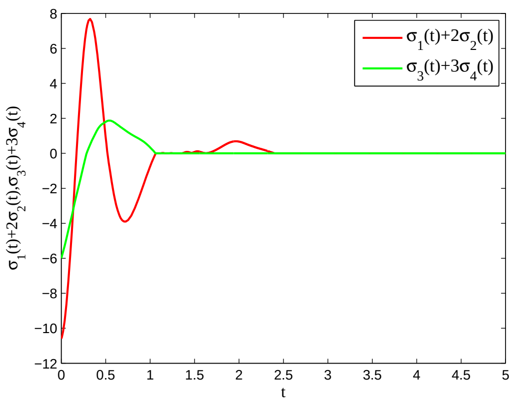

Figure 9: The combination outputs of error signals in clusters 1 and 2 under the second control scheme.

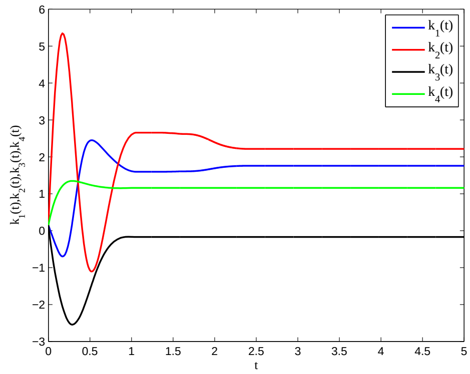

Figure 10: The trajectories of the control gains $k_i, i = 1, .., 4$.

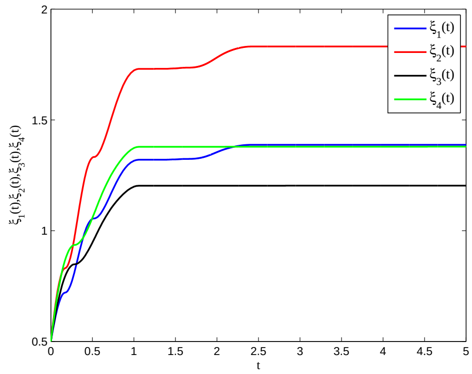

Figure 11: The trajectories of the control gains $\xi_i, i = 1, ..., 4$.

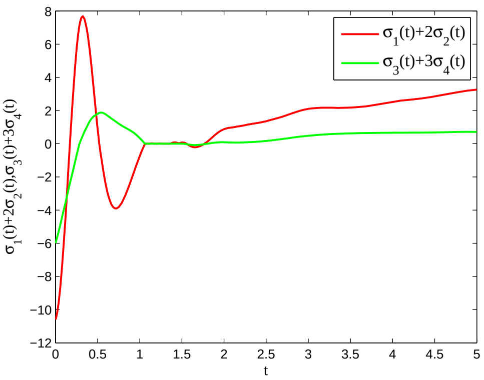

Figure 12: The combination outputs of error signals subject to the attack.

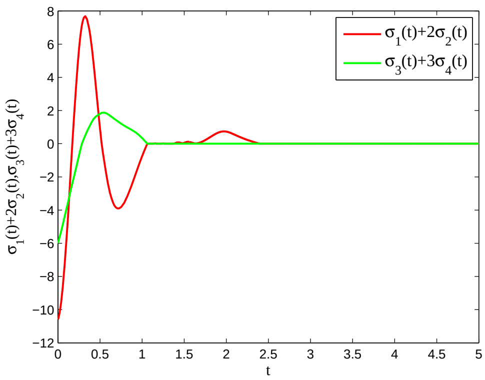

Figure 13: The combination outputs of error signals after the adjustment at the time $t = 1.5$s.

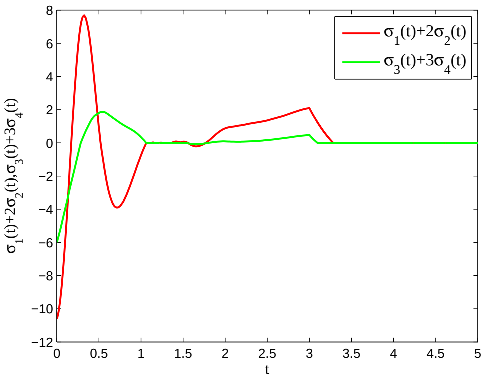

Figure 14: The combination outputs of error signals after the adjustment at the time $t = 3$s.

nodes. Then, the simulation result presented in Fig. 13 indicates that the combination outputs can still tend to zero. If we take $t = 3s$ to make the adjustment, Fig. 14 shows the simulation result, where the combination outputs are clearly reduced and tend to zero from the adjustment instant. These results demonstrate the anti-interference capacity of the control scheme (20).

5. Conclusion

Herein, cluster output synchronization is studied for MNNs, which is distinct from current node-to-node models and provides a more practical model structure for exploring NN synchronization. Two specific control schemes were devised for the proposed model. The first involves designing one feedback controller for each cluster, which saves control costs, and the other involves utilizing multiple adjustable adaptive controllers to decrease control gains and increase the anti-interference capacity of the control system. These two can be flexibly chosen according to specific needs. Simultaneously, a model relationship between MNNs and traditional NNs was established. Via the control schemes, the model relationship and Lyapunov stability theory, sufficient conditions were obtained to guarantee cluster output synchronization. Finally, several simulation examples were employed to illustrate the effectiveness of the proposed model. Although the cluster output synchronization model is first presented, it is still a simplified model for actual operation patterns in NNs. Thus, further developing some more sophisticated models will be a challenging and meaningful topic in the future.

Acknowledgments

This work is supported by The Major Research Project of the National Natural Science Foundation of China (91964108), The National Natural Science Foundation of China (61971185), The Natural Science Foundation of Hunan Province (2020JJ4218), and The Open Fund Project of Key Laboratory in Hunan Universities (18K010).

Compliance with ethical standards

Conflict of interest

The authors declare that they have no conflict of interest.

References

[1] L. Chua, Memristor-the missing circuit element, IEEE Transactions on circuit theory 18 (1971) 507–519.
[2] D. B. Strukov, G. S. Snider, D. R. Stewart, R. S. Williams, The missing memristor found, nature 453 (2008) 80.
[3] K. D. Cantley, A. Subramaniam, H. J. Stiegler, R. A. Chapman, E. M. Vogel, Hebbian learning in spiking neural networks with nanocrystalline silicon tfts and memristive synapses, IEEE Transactions on Nanotechnology 10 (2011) 1066–1073.
[4] C. Wang, H. Xia, L. Zhou, A memristive hyperchaotic multiscroll jerk system with controllable scroll numbers, International Journal of Bifurcation and Chaos 27 (2017) 1750091.

[5] R. Wu, C. Wang, A new simple chaotic circuit based on memristor, International Journal of Bifurcation and Chaos 26 (2016) 1650145.

[6] W. Yao, C. Wang, J. Cao, Y. Sun, C. Zhou, Hybrid multisynchronization of coupled multistable memristive neural networks with time delays, Neurocomputing 363 (2019) 281–294.

[7] Z. Guo, J. Wang, Z. Yan, Attractivity analysis of memristor-based cellular neural networks with time-varying delays, IEEE transactions on neural networks and learning systems 25 (2013) 704–717.

[8] W. Yao, C. Wang, Y. Sun, C. Zhou, H. Lin, Exponential multistability of memristive cohen-grossberg neural networks with stochastic parameter perturbations, Applied Mathematics and Computation 386 (2020) 125483.

[9] Z. Tan, M. Ali, Associative memory using synchronization in a chaotic neural network, International Journal of Modern Physics C 12 (2001) 19–29.

[10] O. A. Heggli, I. Konvalinka, J. Cabral, E. Brattico, M. L. Kringelbach, P. Vuust, Transient brain networks underlying interpersonal strategies during synchronized action, Social cognitive and affective neuroscience (2020).

[11] M. Prakash, P. Balasubramaniam, S. Lakshmanan, Synchronization of markovian jumping inertial neural networks and its applications in image encryption, Neural Networks 83 (2016) 86–93.

[12] Y. Sheng, H. Zhang, Z. Zeng, Synchronization of reaction–diffusion neural networks with dirichlet boundary conditions and infinite delays, IEEE transactions on cybernetics 47 (2017) 3005–3017.

[13] W. Singer, Synchronization of cortical activity and its putative role in information processing and learning, Annual review of physiology 55 (1993) 349–374.

[14] F. C. Hoppensteadt, E. M. Izhikevich, Pattern recognition via synchronization in phase-locked loop neural networks, IEEE Transactions on Neural Networks 11 (2000) 734–738.

[15] Y. Xin, Y. Li, X. Huang, Z. Cheng, Quasi-synchronization of delayed chaotic memristive neural networks, IEEE transactions on cybernetics 49 (2017) 712–718.

[16] N. Li, J. Cao, Lag synchronization of memristor-based coupled neural networks via ω-measure, IEEE transactions on neural networks and learning systems 27 (2015) 686–697.

[17] Y. Feng, X. Yang, Q. Song, J. Cao, Synchronization of memristive neural networks with mixed delays via quantized intermittent control, Applied Mathematics and Computation 339 (2018) 874–887.

[18] X. Yang, J. Cao, J. Liang, Exponential synchronization of memristive neural networks with delays: interval matrix method, IEEE transactions on neural networks and learning systems 28 (2016) 1878–1888.

[19] X. Yang, D. W. Ho, Synchronization of delayed memristive neural networks: Robust analysis approach, IEEE transactions on cybernetics 46 (2015) 3377–3387.

[20] A. Wu, S. Wen, Z. Zeng, Synchronization control of a class of memristor-based recurrent neural networks, Information Sciences 183 (2012) 106–116.

[21] M. Ali, M. Hymavathi, S. Senan, V. Shekher, S. Arik, Global asymptotic synchronization of impulsive fractional-order complex-valued memristor-based neural networks with time varying delays, Communications in Nonlinear Science and Numerical Simulation 78 (2019).

[22] W. Yao, C. Wang, Y. Sun, C. Zhou, H. Lin, Synchronization of inertial memristive neural networks with time-varying delays via static or dynamic event-triggered control, Neurocomputing 404 (2020) 367–380.

[23] V. N. Belykh, G. V. Osipov, V. S. Petrov, J. A. Suykens, J. Vandewalle, Cluster synchronization in oscillatory networks, Chaos: An Interdisciplinary Journal of Nonlinear Science 18 (2008) 037106.

[24] L. Zhou, C. Wang, S. Du, L. Zhou, Cluster synchronization on multiple nonlinearly coupled dynamical subnetworks of complex networks with nonidentical nodes, IEEE transactions on neural networks and learning systems 28 (2016) 570–583.

[25] X. Liu, T. Chen, Finite-time and fixed-time cluster synchronization with or without pinning control, IEEE transactions on cybernetics 48 (2016) 240–252.

[26] J. Cao, L. Li, Cluster synchronization in an array of hybrid coupled neural networks with delay, Neural Networks 22 (2009) 335–342.

[27] L. Li, J. Cao, Cluster synchronization in an array of coupled stochastic delayed neural networks via pinning control, Neurocomputing 74 (2011) 846–856.

[28] P. Liu, Z. Zeng, J. Wang, Asymptotic and finite-time cluster synchronization of coupled fractional-order neural networks with time delay, IEEE transactions on neural networks and learning systems 31 (2020) 4956–4967.

[29] X. Liu, T. Chen, W. Lu, Cluster synchronization in uncertain neural networks through adaptive controllers, Differential Equations and Dynamical Systems 19 (2011) 47–61.

[30] Y. Jimbo, H. P. Robinson, A. Kawana, Strengthening of synchronized activity by tetanic stimulation in cortical cultures: application of planar electrode arrays, IEEE Transactions on Biomedical Engineering 45 (1998) 1297–1304.

[31] L. Zemanová, C. Zhou, J. Kurths, Structural and functional clusters of complex brain networks, Physica D: Nonlinear Phenomena 224 (2006) 202–212.

[32] C. C. Hilgetag, M. Kaiser, Clustered organization of cortical connectivity, Neuroinformatics 2 (2004) 353–360.

[33] T. Tohara, H. Liang, H. Tanaka, M. Igarashi, S. Samukawa, K. Endo, Y. Takahashi, T. Morie, Silicon nanodisk array with a fin field-effect transistor for time-domain weighted sum calculation toward massively parallel spiking neural networks, Applied Physics Express 9 (2016) 034201.

[34] M. Jazayeri, J. A. Movshon, Optimal representation of sensory information by neural populations, Nature neuroscience 9 (2006) 690.

[35] N. J. Majaj, H. Hong, E. A. Solomon, J. J. DiCarlo, Simple learned weighted sums of inferior temporal neuronal firing rates accurately predict human core object recognition performance, Journal of Neuroscience 35 (2015) 13402–13418.

[36] A. Filippov, Classical solutions of differential equations with multi-valued right-hand side, SIAM Journal on Control 5 (1967) 609–621.

[37] J.-P. Aubin, A. Cellina, Differential inclusions: set-valued maps and viability theory, volume 264, Springer Science & Business Media, 2012.

[38] Y. Xu, X. Wu, C. Xu, Synchronization of time-varying delayed neural networks by fixed-time control, IEEE Access 6 (2018) 74240–74246.

[39] C.-J. Cheng, T.-L. Liao, J.-J. Yan, C.-C. Hwang, Exponential synchronization of a class of neural networks with time-varying delays, IEEE Transactions on Systems, Man, and Cybernetics, Part B (Cybernetics) 36 (2006) 209–215.

[40] Z. Fei, C. Guan, H. Gao, Exponential synchronization of networked chaotic delayed neural network by a hybrid event trigger scheme, IEEE

transactions on neural networks and learning systems 29 (2017) 2558–2567.

[41] M. Yoshioka, Cluster synchronization in an ensemble of neurons interacting through chemical synapses, Physical Review E 71 (2005) 061914.

[42] J.-L. Wang, H.-N. Wu, T. Huang, S.-Y. Ren, J. Wu, X.-X. Zhang, Analysis and control of output synchronization in directed and undirected complex dynamical networks, IEEE transactions on neural networks and learning systems 29 (2017) 3326–3338.

[43] J.-L. Wang, H.-N. Wu, Local and global exponential output synchronization of complex delayed dynamical networks, Nonlinear Dynamics 67 (2012) 497–504.

[44] C.-X. Shi, G.-H. Yang, X.-J. Li, Event-triggered output feedback synchronization control of complex dynamical networks, Neurocomputing 275 (2018) 29–39.

[45] Q. Jia, E. S. Mwanandiye, W. K. Tang, Master–slave synchronization of delayed neural networks with time-varying control, IEEE Transactions on Neural Networks and Learning Systems 32 (2020) 2292–2298.

[46] Z. He, C. Li, Z. Cao, H. Li, Periodicity and global exponential periodic synchronization of delayed neural networks with discontinuous activations and impulsive perturbations, Neurocomputing 431 (2021) 111–127.

[47] E. Wu, X. Yang, C. Xu, F. E. Alsaadi, T. Hayat, Finite-time synchronization of complex-valued delayed neural networks with discontinuous activations, Asian Journal of Control 20 (2018) 2237–2247.

[48] B. W. Kernighan, R. Pike, The practice of programming, Addison-Wesley Professional, 2000.

[49] P. J. van der Houwen, B. P. Sommeijer, Iterated runge–kutta methods on parallel computers, SIAM journal on scientific and statistical computing 12 (1991) 1000–1028.

[50] Z. Yang, B. Luo, D. Liu, Y. Li, Adaptive synchronization of delayed memristive neural networks with unknown parameters, IEEE Transactions on Systems, Man, and Cybernetics: Systems (2020).